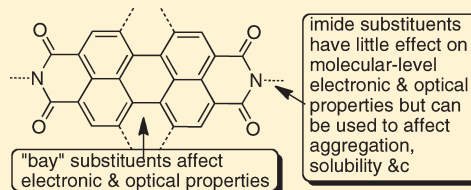# Perylene-3,4,9,10-tetracarboxylic Acid Diimides: Synthesis, Physical Properties, and Use in Organic Electronics

Chun Huang, Stephen Barlow, and Seth R. Marder*

School of Chemistry and Biochemistry and Center for Organic Photonics and Electronics, Georgia Institute of Technology, Atlanta, Georgia 30332-0400, United States

ABSTRACT: Perylene-3,4,9,10-tetracarboxylic acid diimides (perylene diimides, PDIs) have been used as industrial pigments for many years. More recently, new applications for PDI derivatives have emerged in areas including organic photovoltaic devices and field-effect transistors. This Perspective discusses the synthesis and physical properties of PDI derivatives and their applications in organic electronics.

imide substituents have little effect on molecular-level electronic & optical properties but can be used to affect aggregation, solubility &c

"bay" substituents affect electronic & optical properties

1. INTRODUCTION

Perylene-3,4,9,10-tetracarboxylic acid diimide derivatives (also commonly called perylene diimides and abbreviated in this paper as PDIs) have been extensively studied as industrial colorants, both as dyes (soluble) and pigments (insoluble). Figure 1 shows the structure of perylene-3,4,9,10-tetracarboxylic dianhydride (PTCDA), which can be considered as the parent compound of this class of compounds and which was first obtained in the early 1910s,[1,2] and of a generic PDI dye, indicating the numbering of the various positions. PDIs with different chemical and physical properties have been obtained by modification of the substituents, most often those in the imide N,N′ positions and the 1, 6, 7, and/or 12 positions of the hydrocarbon core (the so-called "bay" positions).

PDIs (N,N′-dimethyl PDI, also known as Pigment Red 179, was first reported in 1913[3]) were initially used exclusively as industrial pigments, following the ground-breaking work of Harmon Colors;[1] they constitute a group of high-performance pigments with red to black shades, depending on the fine details of chemical structure and on molecular packing in the solid state.[4] These pigments exhibit excellent chemical, thermal, photo, and weather stability.[1,5] Moreover, paints from PDI-based materials generally show good migration stability after coating on plastics and can be easily overcoated onto other painted surfaces. Accordingly, several PDI derivatives, such as Pigment Red 179, Pigment Red 178, and Pigment Red 149 (Figure 2), have found their way into industrial-scale production and use since early 1950s.[1] Pigment Red 149 is a yellow-shade red material, while Pigment Red 178 and Pigment Red 179 are of blue-shade red color.[1,4,5] Today, PDI-based pigments are used predominately in fiber applications and in high-grade industrial paints, particularly in carpet fibers and in the automobile industry, where their relatively high cost is outweighed by the high quality and/or durability of the colors.[1,5]

However, in addition to their use as important industrial pigments, many PDIs exhibit other interesting properties—such as near-unity fluorescence quantum yields, high photochemical stability, and strong electron-accepting character—that allow PDIs to be used in many other newly developed applications.[5-15] To date, PDIs, as well as related monoimide derivatives, have been utilized in various electronic and optical applications, such as organic field-effect transistors (OFETs),[15-22] fluorescent solar collectors,[23] electrophotographic devices,[24] dye lasers,[11,12] organic photovoltaic cells (OPVs),[16,22,25-28] and optical power limiters,[29,30] due to their specific physical, optical, and/or electronic properties. In many of these applications, the relatively facile and reversible reduction of PDIs plays a key role. These facile reductions, combined with the easily identifiable excited-state, anion, and dianion absorption spectra, have also led to their extensive use in fundamental research on photoinduced energy- and electron-transfer processes.[5,7,31-35] In this paper, the syntheses, physical properties, and the organic electronic applications of PDI derivatives are reviewed.

2. PREPARATION OF PDI DERIVATIVES

2.1. Imidization. In both research and industrial settings, the primary starting material for synthesizing PDI derivatives is PTCDA (Figure 1). The condensation reaction between PTCDA and an alkyl amine or an aniline results in the formation of the appropriate PDI derivative, usually in high yield.[1,5] As shown in Scheme 1, PTCDA is, in turn, obtained industrially through a series of steps beginning with the oxidation of acenaphthene to give 1,8-naphthalene dicarboxylic acid anhydride; this is subsequently treated with ammonia to provide naphthalene-1,8-dicarboxylic acid imide. Perylene-3,4,9,10-tetracarboxylic diimide (PTCDI) is obtained by the oxidative coupling of two of these napthalene imide molecules, for instance, by aerial oxidation in molten potassium hydroxide at ca. 200 °C. PTCDA is then synthesized by hydrolysis of PTCDI with concentrated sulfuric acid at ca. 220 °C. In the dye and pigment industries, insoluble symmetrical organic perylene diimides with high melting points can be easily obtained in high yields from the reactions between PTCDA and various aliphatic amines or anilines.[1] For example,
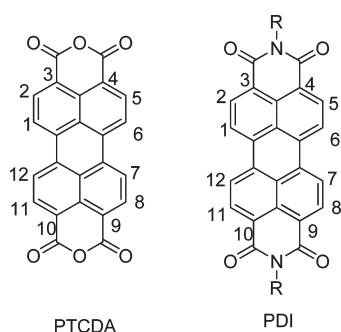
Figure 1. Chemical structures of PTCDA (left) and a generic PDI (right) showing the numbering of the positions in the ring system.
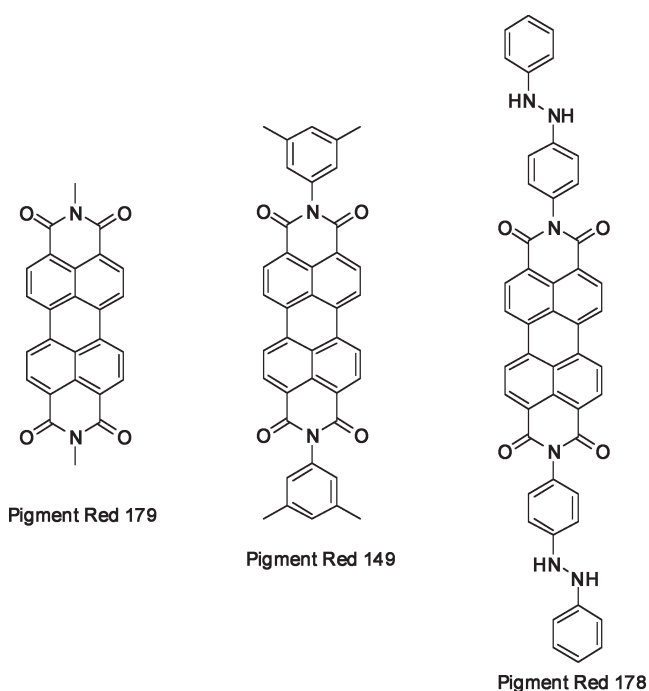

Figure 2. Chemical structures of three PDIs widely used as industrial pigments.

the industrial-scale syntheses of most insoluble PDI pigments, such as Pigment Red 179, Pigment Red 178, and Pigment Red 149, afford yields of over 90% from PTCDA and the respective amines or anilines.[36,37]

Although insoluble and high-melting PDI-based materials are required for the pigment industry, current work on PDIs for organic electronics, studies of photoinduced processes, and supramolecular organization generally requires PDIs with reasonable solubility in common solvents.[5] Consequently, synthetic methods for highly soluble PDIs have been developed using substitution at the imide positions and/or in the bay positions (see section 2.2). The first and most commonly employed approach to organic-soluble symmetrical PDIs, first described by Langhals and co-workers in the 1990s, is to use solubilizing alkyl or aryl substituents at the PDI imide positions.[38] So-called "swallowtail" substituents[39]—long alkyl chains attached to the imide nitrogen atom through their central positions, such as 10-nonadecyl groups—and *ortho*-substituted *N*-aryl groups[40] are particularly effective solubilizing groups; the bulky

Scheme 1. Preparation of PTCDA and *N,N′*-Disubtituted PDIs
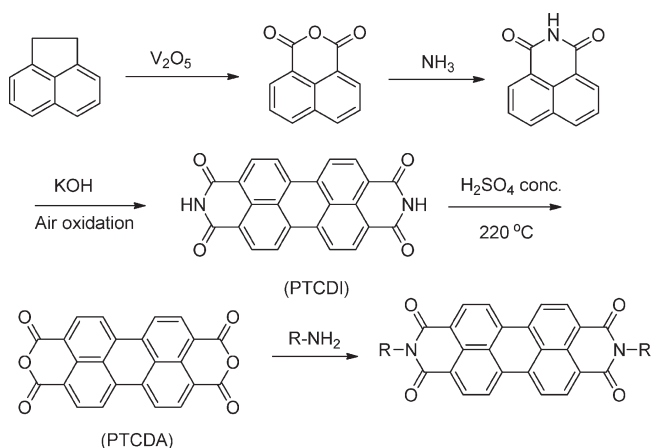

substituents are forced out of the plane of the PDI chromophore, thereby limiting the face-to-face $\pi-\pi$ stacking of the PDI molecules.[5,39,40] Halogenated solvents, such as dichloromethane, chloroform, and chlorobenzene, are typically good solvents for *N,N′*-dialkyl and diaryl PDI derivatives of this type. Water-soluble PDIs have been obtained by incorporating hydrophilic moieties, including Newkome-type carboxylates,[41] phosphate surfactants,[42] polyglycerol dendrons,[43] and cyclodextrin,[44] into the substituents the imide positions. It is worth noting that nearly all PDI pigments can be dissolved in concentrated sulfuric acid via protonation and can be recovered by diluting the acid solution with water.[45]

Soluble symmetrically *N,N′*-substituted PDIs are commonly obtained by the condensation reaction of PTCDA with anilines and aliphatic primary amines at high temperatures (>160 °C) in solvents such as molten imidazole or quinoline with anhydrous zinc acetate (typically 10−30 mol %) as a catalyst (Scheme 2). In many cases, isolated yields approach 95%, and the products are relatively easily purified.[5,38,45] Alternatively, the treatment of PTCDA (or analogues with dibromo or tetrachloro substitution of the "bay" positions) with primary amines in hot alcohols (such as *n*-butanol), carboxylic acids (such as acetic acid and propionic acid), or alcohol/water mixtures (such as 1:1 *n*-butanol/water) can give isolated yields over 90%.[45] Furthermore, benzoimidazole derivatives can also be obtained via condensation of PTCDA and *o*-phenylenediamine derivatives in good to excellent isolated yields, generally as a mixture of two regioisomers (Scheme 2) that are not easily separated, either by column chromatography or recrystallization.[37,45,46]

Unsymmetrical PDIs with different substituents on each imide position have also been reported. Attempts to obtain compounds of this type from PTCDA with either simultaneous or sequential addition of two different amines are usually unsuccessful because of differences in reactivity of the amines with PTCDA. Typically, only traces of the desired products are observed, with the dominant species being the two symmetrical PDIs.[45] Accordingly, PDIs of this type must usually be synthesized using more complex multistep methods.[45] One such method (Scheme 3, method A) relies on partial hydrolysis of symmetrical PDIs to perylene monoimide monoanhydride compounds, a reaction that gives yields of ca. 50%. Imidization of the mixed imide-anhydride with a second amine or aniline provides the

Scheme 2. Conversion of PTCDA to Dialkyl and Diaryl PDIs (Top) and to Perylene Benzoimidazole Derivatives (Bottom)
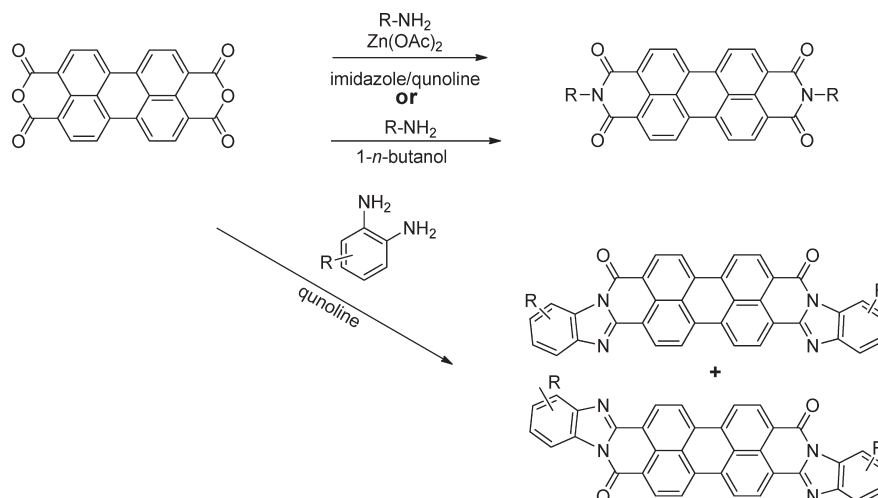

Scheme 3. Two Methods for the Preparation of Asymmetrical PDIs with Different Substituents on Each Imide Position
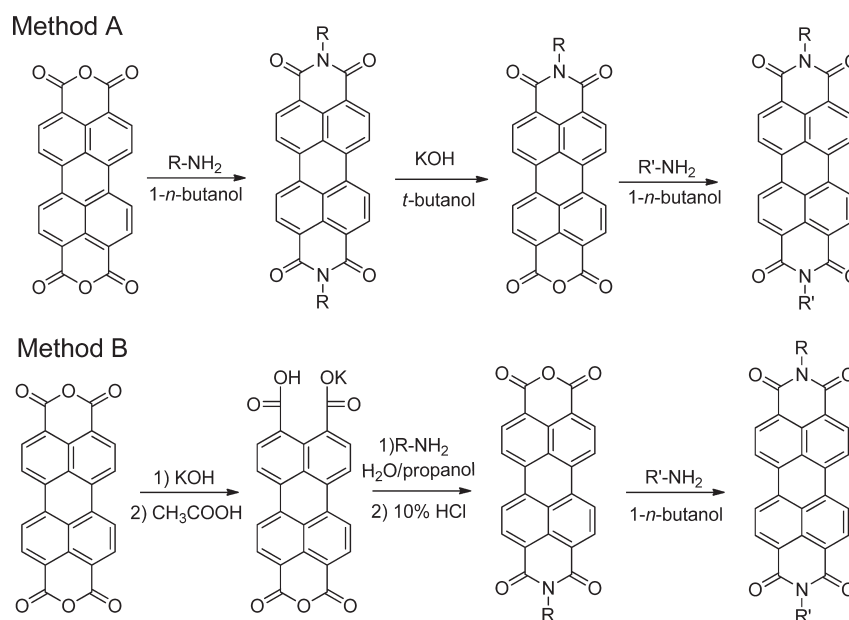
desired asymmetrical PDI. A mixed imide—benzoimidazole has also been prepared from a mixed imide—anhydride with an o-phenylenediamine derivative.[47] It should be noted that the direct synthesis of perylene monoanhydride monoimide compounds directly from imidization of PTCDA is typically challenging; generally, diimides are the predominant products, even when 1 equiv or less of a primary amine is used, presumably due to the increased solubility of the intermediate mixed imide—anhydride relative to that of PTCDA. Another practical approach to asymmetrical PDI synthesis was first described by Tam-Chan and co-workers in the late 1990s (Scheme 3, method B);[48] partial hydrolysis of PTCDA to a mixed anhydride—dicarboxylate salt was followed by successive imidization reactions. However, method A is more widely utilized because it typically provides the desired material in higher yield and purification is usually easier.[17,49−52]

2.2. Substitution in the Bay Positions. The introduction of aryl or aryloxy groups into the 1, 6, 7, and/or 12 (bay) positions of PDIs can be used to increase solubility, the substituents being forced out of the PDI plane by steric interactions. Moreover, these groups, as well as smaller substituents, such as bromo, can lead to the twisting of the two naphthalene half units in PDIs. Both effects disrupt face-to-face π−π stacking and improve the solubility of PDIs. Incorporation of bulky groups into the bay positions can increase the solubility by several orders of magnitude;[53] for example, 1,(6)7-dibromo N,N'-dioctyl PDI shows reasonable solubility in common organic solvents, while its unbrominated analogue is insoluble in most organic solvents. As will be discussed in more detail in section 3, bay substituents can also be used to significantly modify the molecular-level electronic and optical properties of PDIs. As shown in Scheme 4, tetrachloro

Scheme 4. Preparation of PDIs with Various Substituents in the Bay Positions[a]
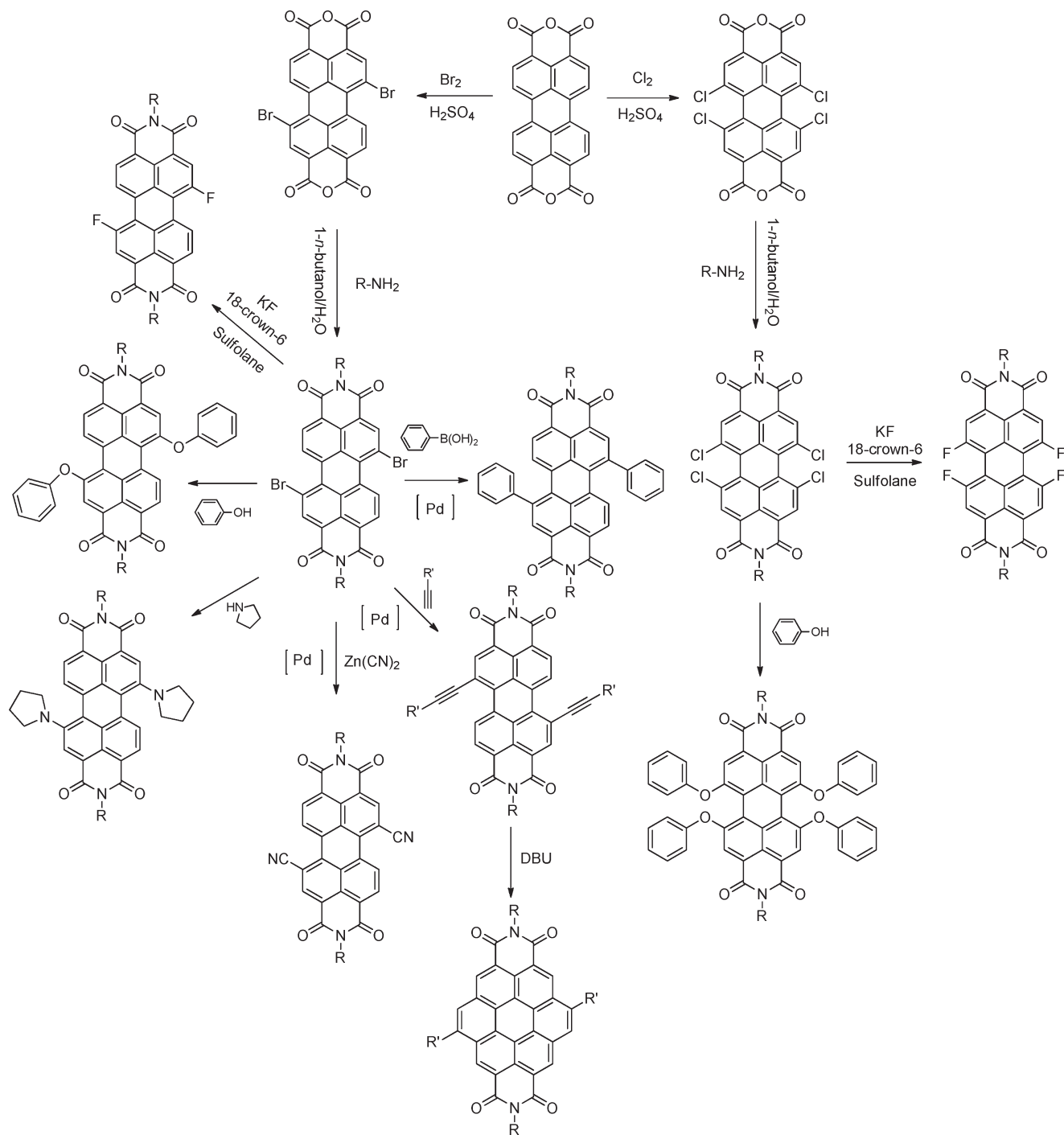
[a] Note that formation of 1,7-disubstituted derivatives shown is typically accompanied by formation of the corresponding 1,6-disubstituted derivatives (not shown).

and dibromo derivatives of PDIs are key intermediates for the synthesis of a wide range of other bay-substituted derivatives and are generally obtained by imidization of the corresponding halogenated PTCDA derivatives. The procedure for the tetrachlorination of PTCDA with sulfuric acid and chlorine appeared in literature in 1980s.[54] Solubilizing substituents were introduced into the bay positions by Seybold and co-workers at BASF in the late 1980s;[5,55] 1,6,7,12-tetraphenoxy PDIs were obtained after

heating the corresponding tetrachloro species with phenol and potassium carbonate in N-methylpyrrolidone.[56] More recently, the reaction of 1,6,7,12-tetrachloro PDIs with potassium fluoride in sulfolane at elevated temperature in the presence of a catalyst ((N,N-dimethylimidazolidino)tetramethylguanidinium chloride or 18-crown-6), has been used to synthesize the corresponding tetrafluoro derivatives; zero to moderate yields are obtained, depending on the imide substituents and the choice of catalyst.

Scheme 5. Preparation of Pyridine-Annulated PDIs
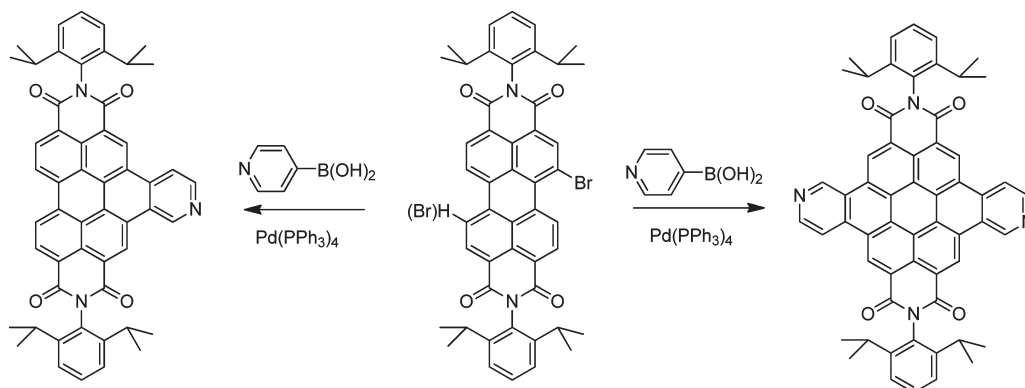
The resulting fluoro derivatives have been used as electron-transport materials in OFETs.[57,58]

Conditions have also been developed for the bromination of PTCDA[59] to give predominantly a mixture of 1,6 (minor, ca. 10−20%) and 1,7 (major) regioisomers of the dibromo product (as indicated by conversion of the crude insoluble reaction product to soluble PDIs); mono- and tribrominated side products are also obtained. Mono-, di-, and tribrominated PDIs can generally be separated by column chromatography, but the two dibromo PDI regioisomers are often very challenging to separate and can only be distinguished from one another using high-field (>400 MHz) ^{1}H NMR spectroscopy.[5,60] Some derivatives have, however, been obtained, albeit in low yield, as the pure 1,7-dibromo isomers after multiple recrystallizations.[5,60] More aggressive bromination conditions for PTCDA have also been used to obtain the 1,6,7,12-tetrabromo derivative, which can be imidized to tetrabromo-PDIs.[61,62] Recently, it was discovered that PDIs can be directly dibrominated using bromine at room temperature in solvents such as dichloromethane, although, as with bromination of PTCDA, mono- and tribrominated products can be obtained, as well as both 1,6- and 1,7-dibromo species. This method has also been successfully in preparing monobromo-PDIs.[63] More forcing bromination conditions, such as heating to ca. 50 °C, can give the dibromo-substituted PDIs (isomeric mixture) as the dominant products in good yields (>90% for some cases) and shorter reaction times.[30,63]

Nucleophilic substitution of bromo bay substituents is relatively straightforward, and generally, products can be isolated in relatively high yields; as shown in Scheme 4, fluoride-,[57] cyanide-,[18,64] phenol-,[38] and amine-based nucleophiles[65] have been coupled to dibromo-PDIs, leading to PDIs with a variety of optical and electronic properties due to the significant electronic coupling between the substituents and the PDI cores (see section 3). Moreover, dibromo-PDIs have also been used in transition-metal-catalyzed C−C couplings, such as Suzuki,[66,67] Stille,[16,68] and Sonogashira reactions,[33,69] to obtain various aryl-, heteroaryl-, and alkynyl-functionalized PDIs. Products from both nucleophilic substitution and palladium-catalyzed reactions are typically obtained, and often studied and used, as mixtures of isomers due to the use of a mixture of 1,6- and 1,7-dibromo PDIs; however, in some cases, for example, where the bay substituents are bulky triphenylsilylalkynyl groups, 1,6-, and 1,7-isomers can be separated via column chromatography.[19] 1,6,7,12-Tetrabromo-PDIs have also been converted to 1,6,7,12-tetraphenyl-PDIs using the fluoride ion-mediated and Ag$_2$O-promoted Suzuki coupling reaction.[67]

The base-catalyzed cyclization of 1,7-dialkynyl-PDIs obtained from Sonogashira couplings has been used to expand PDIs to coronene-2,3,8,9-tetracarboxylic acid diimides.[69−71] Recently, a facile one-pot synthesis of pyridine-annulated PDIs from mono- or dibromo-PDIs was reported by Wang and co-workers; as shown in Scheme 5, the synthesis combines a Suzuki coupling with a subsequent photoinduced cyclization.[72] Copper-mediated oligomerization of 1,6,7,10-tetrachloro- or tetrabromo-substituted PDIs can, in principle, give graphene-like ladder polymers.[73−75] Oligomeric derivatives, including systems containing two, three, or four PDIs (with varying degrees of dehalogenation of the open bay positions of the terminal PDI units), have been isolated in low yields from reactions of this type. As shown in Scheme 6 for the case of the trimeric species,[59] different structural isomers are possible; however, in both trimeric and tetrameric systems isomers have been successfully separated using HPLC.

Substitution in Other Positions. Syntheses of 2,5,8,11-substituted PDIs have not been reported until very recently, when ruthenium-catalyzed C−H bond activation was found to be effective for direct arylation[76] or alkylation[77] of perylene diimides at these positions, as illustrated in Scheme 7. The introduction of alkyl groups at these positions significantly enhances the solid-state fluorescence quantum yield relative to those of unsubstituted analogues. Good solubility in organic solvents can also be achieved and, in contrast to solubilization through bay substitution, is not accompanied by serious distortion of the PDI cores from planarity;[77] this feature may be beneficial for applications in solution-processed OFETs where strong $\pi-\pi$ stacking can lead to effective electronic coupling between molecules. Both electron-rich and electron-poor aryl groups can be incorporated in satisfactory yields. More recently, 1,2,5,6,7,8,11,12-octachloro-perylene-3,4:9,10-tetracarboxylic acid diimide was synthesized in high yield by chlorination of PTCDI in chlorosulfonic acid at 80 °C, as shown in Scheme 8. However, due to the limited solubility of this material, multiple recrystallizations and gradient sublimation were necessary to obtain material with sufficient purity for OFET applications.[78]
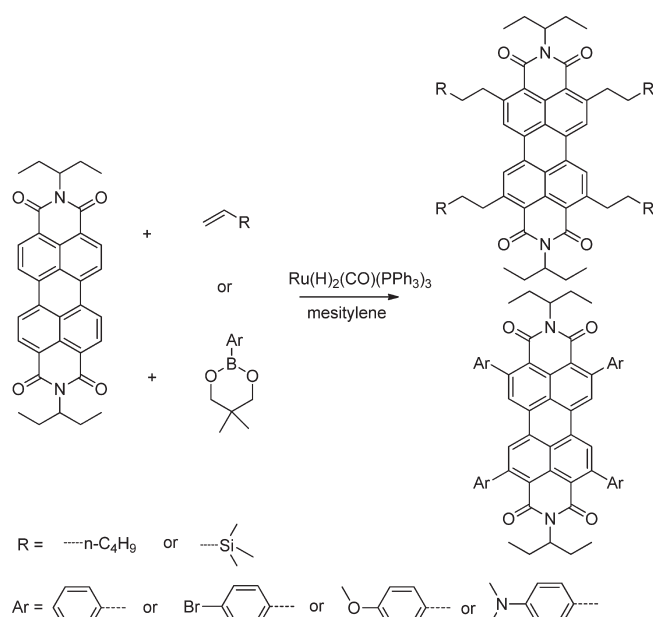
3. PHYSICAL PROPERTIES OF PDIS

3.1. Absorption and Fluorescence. In the absence of aggregation effects, the lowest energy electronic transitions of typical N,N'-dialkyl or diaryl PDIs without substituents on the perylene
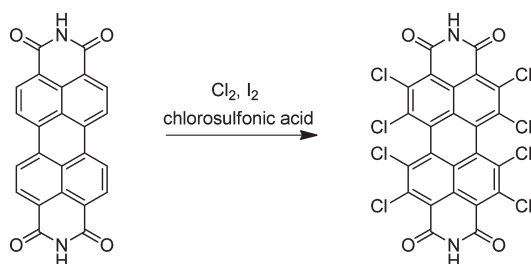
Scheme 6. Preparation of Annulated Ter(PDI) Derivatives
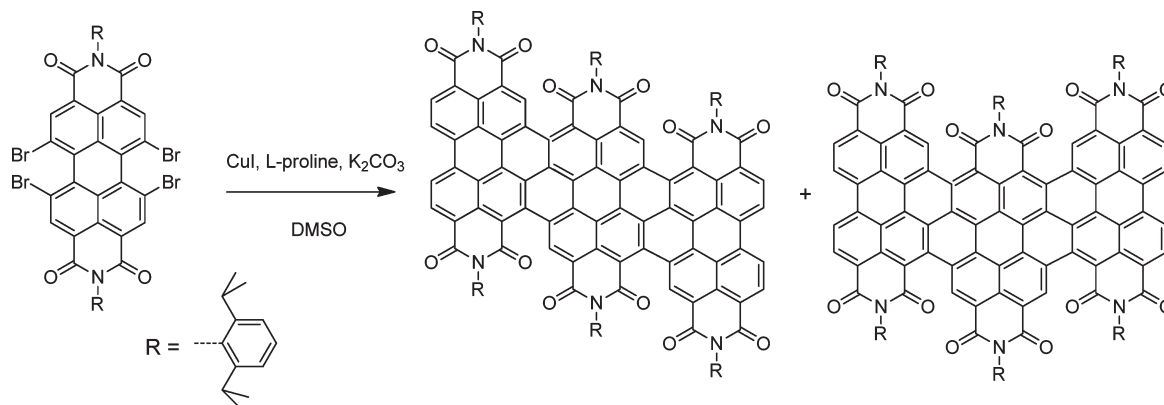
Scheme 7. Preparation of 2,5,8,11-Substituted PDIs

Figure 3. UV−vis absorption (solid line) and emission (dashed line) spectra of a typical PDI in toluene.

shift and appears as a mirror image of the absorption spectrum in solvents such as toluene and chloroform.[5] In many cases, the fluorescence quantum yields are almost unity (see Table 1 for examples), and the singlet excited-state lifetimes are rather long (approximately 4 ns in common organic solvents).[5,12,26,45,79] These long excited-state lifetimes have been exploited in two-photon-induced optical-limiting applications in the NIR.[29,80] INDO calculations indicate that the $S_0 \rightarrow S_1$ transition is well described as a HOMO→LUMO excitation.[81] The DFT-calculated HOMO and LUMO of a simple PDI are shown in Figure 4 and similar to those previously obtained using a variety of computational methods (for example, the Hückel orbitals shown in ref 4). The symmetries of these orbitals mean that the optical transition is polarized along the long molecular (N−N) axis. The orbitals also show that the nitrogen atoms are located on nodal planes of both HOMO and LUMO; accordingly, the effects of imide substitution on the frontier orbital energies are expected to be inductive in nature and, therefore, similar for both HOMO and LUMO, leading to little change in the optical properties. This is indeed the case; absorption and emission maxima generally vary by ca. <5 nm with variation of N,N′ aryl or alkyl substituents.[45] The spectra of benzoimidazole-annulated derivatives, such as those shown in Scheme 2, are, however, significantly bathochromically shifted relative to those of simple PDIs, consistent with more extensive

Scheme 8. Preparation of 1,2,5,6,7,8,11,12-Octachloro PDI

core are strong vibronically structured absorptions with maxima at ca. 525 nm and peak absorptivities approaching 10^5 M^{-1} cm^{-1}. Figure 3 shows a typical example, along with the corresponding fluorescence spectrum, which typically exhibits only a small Stokes
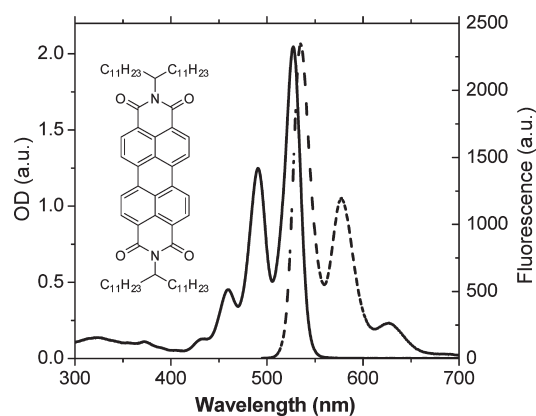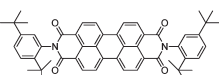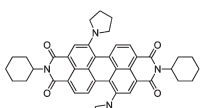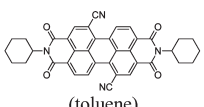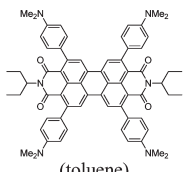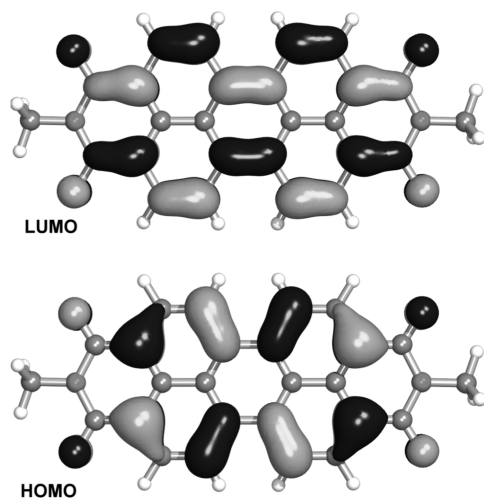
Table 1. Absorption and Fluorescence Maxima, Peak Absorptivities, and Fluorescence Quantum Yields of Selected PDIs

Compound (solvent)	$\lambda_{abs\text{-}max}$ / nm	ε_{max} / $M^{-1}cm^{-1}$	$\lambda_{em\text{-}max}$ / nm	Φ_F / %	Ref
(CH$_2$Cl$_2$)	526	88000	533	100	79
(CH$_2$Cl$_2$)	526	94000	537	100	12
(toluene)	686	46000	721	35	65
(toluene)	530	47000	545	100	10,18
(toluene)	528	59000	--	--	76

Figure 4. Frontier orbitals of *N,N'*-dimethyl PDI, according to DFT calculations.

delocalization of the HOMO onto the terminal arylene group shown by MO calculations.[80,82]

Core substitution can significantly affect both the absorption and emission properties of PDIs. As shown in Figure 4, there are significant HOMO and LUMO coefficients on the bay positions (and also at the 2, 5, 8, and 11 positions); accordingly, the HOMO is expected to be destabilized by π-donor substituents and the LUMO stabilized by π-acceptors, leading to bathochromic shifts of the spectra in either case. Although, in many cases, steric effects imparted by bay substituents can lead to a twisting of the PDI core, potentially leading to an hypsochromic shift, the above-mentioned effects often dominate. For example, the absorption

and emission spectra of PDIs with 1,7-diphenoxy π-donor substituents retain some of the vibronic structure seen for analogous PDIs without bay substituents but are bathochromically shifted by ca. 20 and 40 nm, respectively. Accordingly, the color of the fluorescence changes from yellow or yellow-green to orange.[5,83] Stronger π-donors, such as pyrrolidino groups,[30,65] lead to even more significant shifts; 1,7-dipyrrolidino PDIs appear dark green in both the solid sate and solution due to a bathochromic shift of over 150 nm relative to unsubstituted analogues. In compounds of this type, the optical transition acquires significant amino-to-PDI quadrupolar charge-transfer character and, accordingly, these compounds are somewhat solvatochromic; their fluorescence quantum yields are also significantly decreased (Table 1).[5,19,65] Fluoro, chloro, and bromo substituents lead to bathochromic shifts of only a few nanometers, and no significant charge-transfer character is observable,[5,57,60,64] consistent with their weak π-donor character. Cyano substituents also lead to similar behavior, despite their π-acceptor character, presumably due to a large energy mismatch between the PDI- and CN-localized empty orbitals, leading to only a small differential stabilization of the LUMO relative to that of the HOMO. As shown in Table 1, fluorescence quantum yields remain high for cyano derivatives.

Incorporation of extended conjugated groups in the bay positions also generally leads to bathochromically shifted spectra. Retention of vibronic structure is seen in the case of aryl and arylethynyl groups bearing various para substituents varying from π-acceptors to the moderately π-donating alkoxy group.[33,34,84] Rather different spectra are seen in the case of stronger donor substituents such as *p*-aminophenyl, (*p*-aminophenyl)ethynyl, and oligothiophene-based moieties; these spectra consist of a band in the range ca. 460−530 nm, often with discernible vibronic structure, and a broad structureless band at considerably longer wavelength (ca. 600−720 nm).[33,34,84−86] Molecular orbital
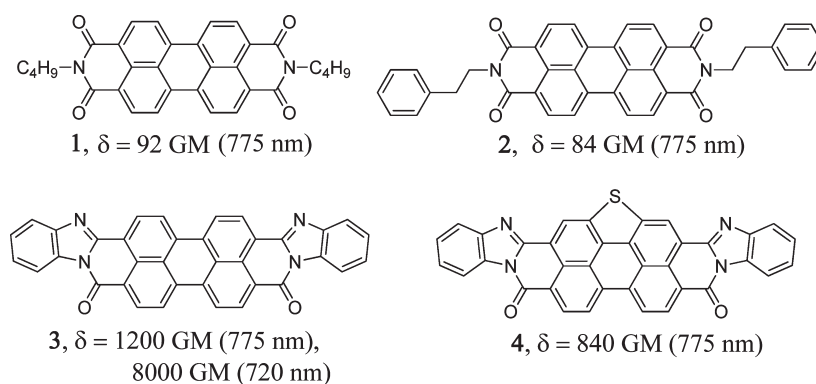
Figure 5. 2PA cross-sections for some PDIs measured in dichloromethane containing 10% using the fs Z-scan technique.[80,82,93]
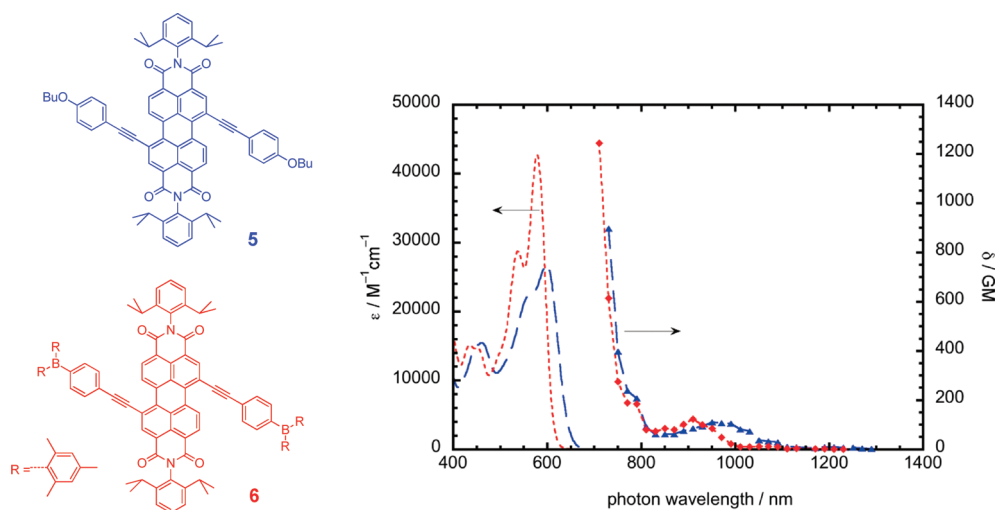

Figure 6. One-photon absorption (lines) and 2PA spectra (lines with data points) of two bay-substituted PDI derivatives (**5** (blue) and **6** (red)) in solution (toluene); the 2PA spectra were recorded using the two-photon-induced fluorescence method. Reprinted with permission from ref 33. Copyright 1994 American Chemical Society.

calculations indicate that the HOMOs of these species are primarily localized on the donor substituents, while the LUMOs are similar to those of simple PDIs;[34,84−86] thus, the low energy bands presumably have much stronger donor-to-PDI charge-transfer character than those of the bis(pyrrolidino) species, while the higher energy vibronically structured bands are likely to be PDI-localized transitions. Similar spectra are also observed for alternating conjugated donor−acceptor polymers based on PDIs linked by various oligothiophene-type bridges through their bay positions.[16,27,68,87−89] Compounds of this type also exhibit rather low fluorescence quantum yields[84−86] and short excited-state lifetimes.[33,85,86]

The electronic nature of aryl substituents in the 2,5,8,11-positions also has a significant impact on the optical properties of PDIs.[76] For example, a PDI with p-(N,N-dimethylamino)phenyl groups in the 2,5,8,11-positions exhibits a broad band around 600−700 nm. Moreover, the fluorescence quantum yields of 2,5,8,11-donor-substituted PDIs are much lower than the parent PDIs (for example, approaching zero for a tetrakis(p-(N,N-dimethylamino)phenyl)-substituted example and close to unity for an unsubstituted analogue).[76]

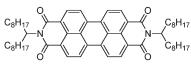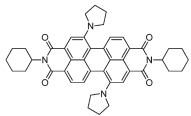Annulation of the perylene core can have a variety of effects on the optical properties of PDI-related species: relative to the spectra of simple PDIs those of coronene diimides are significantly hypsochromically shifted,[70,90] those of the pyridine-fused species shown in Scheme 5 are essentially unaffected,[72] and the spectra of the ladder oligomers shown in Scheme 6 are complex with the lowest energy transitions being significantly bathochromically shifted.[74,75]
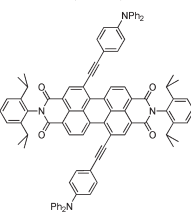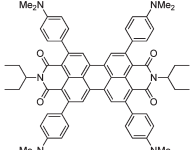
As noted in previous sections, PDIs are prone to π-stacking. In solution, such aggregation effects typically lead to changes in the vibronic structure of absorption and fluoresence absorption bands. In the spectra of nonaggregated PDIs with only N,N' substituents (such as that shown in Figure 3), the ratio of the absorptivity of the 0,0 band at ca. 527 nm to that of the 0,1 vibronic band at ca. 490 nm is greater than 1.6;[91] aggregation causes a significant decrease in this value and also has similar effects on the emission.[12,91,92] As a consequence of the propensity for aggregation, the optical properties of PDI-based dyes, including both simple dyes and bay-substituted examples, are, in general, strongly dependent upon concentration and on environmental conditions such as solvent polarity and temperature.

The two-photon absorption (2PA) spectra of PDIs and related chromophores have also been examined.[33,80,82,93] In general, the spectra are dominated by the onset of rather strong 2PA (cross-sections >1000 GM; 1 GM = 10^{-50} cm^4 s (photon)$^{-1}$) as the

Table 2. Half-Wave Redox Potentials (V vs Ferrocenium/Ferrocene) for Some PDIs

| Compound (solvent)	$E_{1/2}^{-/2-}$	$E_{1/2}^{0/-}$	$E_{1/2}^{+/0}$	Ref
(MeCN)	−1.21	−0.98	+1.21	79
(PrCN)	−1.46	−1.28	+0.16	65
(PrCN)	−0.92	−0.59	−	10,18
(CH₂Cl₂)	−1.21	−0.92	+0.61[a]	33
(CH₂Cl₂)	−1.41	−1.31	−	76

[a] Presumably correspons to triarylamine-based oxidation, rather than being PDI-centered.

photon energy approaches that of the lowest energy one-photon transition, suggesting that a two-photon-allowed state lies at an energy close to twice that of the one-photon state. This small detuning energy between the photon energy and one-photon state energy can largely explain the large cross-sections observed for these compounds. Simple PDIs (**1** and **2** in Figure 5), benzoimidazole-annulated examples (**3** and **4** in Figure 5), and 1,(6)7-di(phenylethynyl) derivatives (**5** and **6** in Figure 6) all show peaks or shoulders corresponding to excitation into a state at ca. 1.5 times the energy of the low-lying one-photon state;[33,80,82] however, the cross-sections for this feature vary with the details of the structures, values of ca. 1000, 4000, and 200 GM being reported for examples of these three classes of compounds, respectively. Compounds **3** and **4** both show large cross-sections over a relatively wide spectral region; overlap with their excited-state absorption spectrum allows their use for optical limiting at ca. 770 nm.[80] Compounds **5** and **6** also show well-defined 2PA maxima at much longer wavelengths (peak cross-sections of 100−150 GM at ca. 900−960 nm).[33]

3.2. Redox Properties. Electrochemical data for some representative PDIs are summarized in Table 2.[5,64,65,94,95] As shown in Table 2, for typical simple N,N'-dialkyl or diaryl PDIs without core substitution two reversible reduction waves (at ca. −1.0 and −1.2 V vs FeCp$_2^{+/0}$) and one reversible oxidation wave (at ca. +1.2 V) can be observed in appropriate organic solvents. The identity of the N,N' substituents has little effect on the redox potentials; even replacing N,N'-diphenyl substituents by

electron-withdrawing N,N'-di(pentafluorophenyl) groups increases the ease of reduction by only 0.11 V.[5,20] As with the effects of these substituents on optical data, their moderate effect on redox potentials can be related to the location of the imide nitrogen atoms on a nodal plane in the LUMO (and HOMO) (see Figure 4), the orbital energies being modified by inductive effects relayed via the imide nitrogen atoms. Conversely, substituents on the core can have pronounced effects on the redox potentials.[5,10,18,66] For example, PDIs with strongly electron-withdrawing cyano or fluoro substituents in the bay positions are 0.3−0.4 V more easily reduced than analogues without bay substituents and are also less readily oxidized;[5,64] these changes in redox properties are primarily due to the inductive effect of these groups on the frontier orbitals, both of which have significant coefficients on the directly attached carbon atoms. Derivatives with π-donating pyrrolidino substituents in the bay positions are some 0.3 V less readily reduced and ca. 1.0 V more readily oxidized than analogues without bay substituents.[5,65,94] PDI derivatives with arylethynyl bay substituents are generally slightly more readily reduced compared to unsubstituted perylene diimides, regardless of whether the aryl groups bear π-donor or π-acceptor groups, indicating some delocalization of the LUMO onto the conjugated substituents.[33]

Substituents in the 2,5,8,11-positions also significantly affect the redox properties of PDIs.[76] In general, electron-donating aryl groups lead to a cathodic shift of the reduction potential while acceptors make cause an anodic shift of the reduction potential.
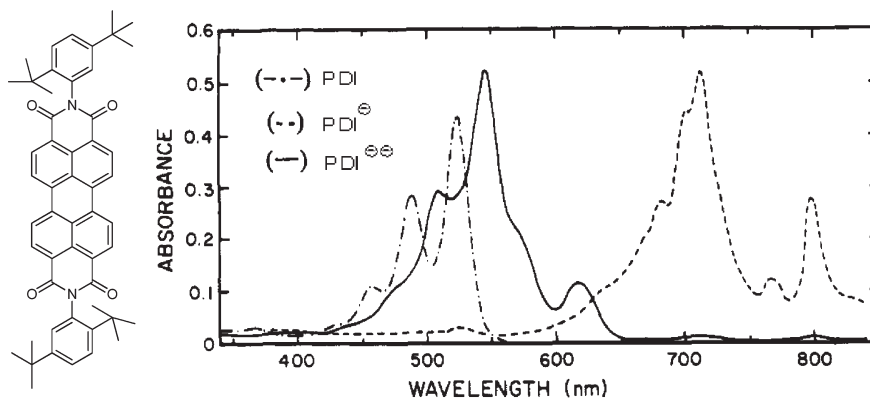
Figure 7. PDI anion and dianion absorption in ethanol (containing 1×10^{-4} M tetramethylammonium hydroxide) obtained by controlled reduction with H_2 in the presence of Pt. Reprinted with permission from ref 98. Copyright 1989 American Chemical Society.

For example, incorporation of *p*-(*N,N*-dimethylamino)phenyl groups on the 2,5,8,11-positions leads to a first reduction potential at around 0.2 eV less reducing potential than that of the parent PDIs.[76] On the other hand, a *p*-(trifluoromethyl)phenyl analogue is around 0.17 eV more readily reduced than the parent PDI.[76]

The optical spectra of the radical anions and the dianions formed by reduction of PDIs are generally well-characterized. In part, this is due to the reasonable stability of these species and the ease with which they can be generated; for example, PDI anions have been generated through photoreduction in presence of triethylamine,[96] electrochemical reduction,[97] by platinum-catalyzed reduction with hydrogen,[98] and using cobaltocene.[33] In addition, as discussed below, PDI derivatives are widely used in transient absorption studies of photoinduced electron-transfer (see below), and anion and dianion spectra can give insight into the origin of features observed in the transient spectra. The absorption spectra of a neutral PDI and its chemically generated anion and dianion are shown in Figure 7 (radical anions of PDIs such as this also typically exhibit a third transition at still longer wavelength, not shown in Figure 7). The peak molar absorption coefficient for the PDI radical anion at 713 nm is ca. 1.0×10^5 M^{-1} cm^{-1}, while the dianion shows an absorption coefficient of ca. 1.0×10^5 M^{-1} cm^{-1} at the 546 nm peak. As with neutral PDIs, substituents at the imide positions have limited impact on position and strength of the anion absorption spectra, while substituents in the bay region cause considerable change in the band shapes and peak positions.[31,33,98] Nonetheless, the radical anion spectra of a wide variety of PDI derivatives are typically recognizable due to the presence of three relatively sharp transitions in the visible to NIR region, enabling one to readily follow the dynamics of electron-transfer processes in functionalized PDIs using transient-absorption techniques.[31,99,100]

3.3. Solid-State Structures and Self-Assembly. The molecular packing behavior of PDIs in the solid state has been extensively studied since the early 1980s in order to understand how to control the colors of PDI pigments for industrial applications.[1,4,5] Crystal structures reveal that the flat PDI cores generally form π-stacks in which the principal axes of the molecules are parallel to one another and in which the interplane distance is ca. 3.4 Å, similar to the interlayer distance in graphite.[5,17,101,102] Substituents at the imide positions can significantly affect the stacking behavior, including the longitudinal and transverse offset between the neighboring dyes in the solid state, significantly influencing the intermolecular interactions of

the π-systems in the crystal lattice and so leading to colors in the solid state varying from red to nearly black.[5,103] On the other hand, bay substitution often causes a distortion of the π-systems from planarity due to intramolecular steric interactions; this often significant disrupts the π-stacking of PDIs, especially in the solid state.[13,78,104] More recently, the packing of solid PDIs has also been studied in the context of organic electronics applications (see below), where good intermolecular orbital overlap is related to charge-carrier mobility.[78,105] Moreover, as discussed in section 4.1, the manner in which *N,N'*-substituents fill space in the structure has also been used to explain the air-stable electron transport observed in PDIs with fluoralkyl imide substituents.[20,106]

Another area of increasing interest focuses on the supramolecular organization of PDI derivatives using interactions including π−π stacking, hydrogen bonding, and/or metal−ligand-coordination to form functional molecular architectures.[5,107,108] New materials with interesting optical and electrical properties have been demonstrated by Müllen, Würthner, Meijer, and others using PDI-based materials.[4,100,107,109−111] Examples of metal-coordination-directed and hydrogen-bonding-directed self-assembly in forming PDI-based supramolecular structures are shown in Figure 8.[110,112,113] Currently, nanostructures and even larger assemblies with appealing physical chemical and/or biological properties have become accessible using functionalized PDIs. More importantly, the use of supramolecular organization in preparing such nanoarchitectures from relatively simple molecules is potentially less time-consuming relative to multistep organic synthesis as a route to functional materials. An excellent in-depth discussion of the supramolecular organization of PDIs by Würthner can be found in the literature.[5]

3.4. Photoinduced Electron Transfer. Photoinduced electron-transfer (ET) reactions involving PDIs, primarily as electron acceptors, have been widely studied. Both intermolecular ET between PDI-based acceptors and electron donors, such as polythiophenes, and intramolecular ET within covalently linked donor−PDI molecules have been extensively studied using transient absorption spectroscopy,[8,19,31,34,114] typically taking advantage of the easily identifiable radical-anion or dianion absorptions of PDIs discussed in section 3.2. Such research provides insight into the fundamental physical chemistry of photoinduced electron-transfer, as well as being relevant to the development of technologies utilizing photoinduced ET to PDI-based materials, such as OPVs[34,85,114] and charge-transfer-based optical limiting.[30]
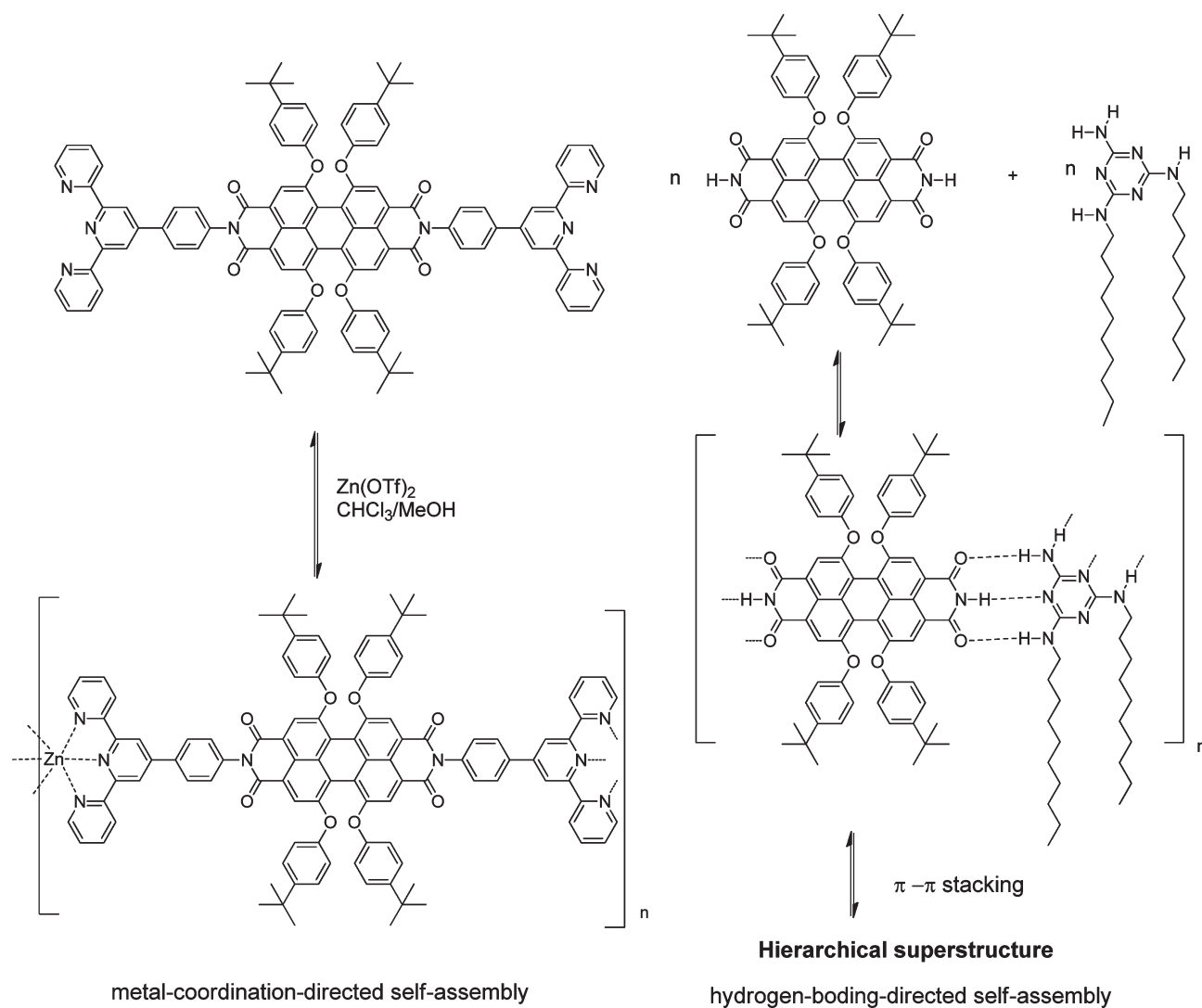
Figure 8. Metal-coordination-directed (left) and hydrogen-bonding-directed (right) self-assembly in forming PDI-based supramolecules.
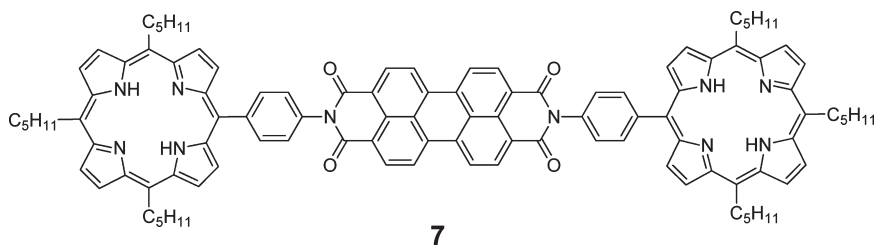
Figure 9. Example of a porphyrin–PDI–porphyrin triad.

Photoinduced ET in systems containing porphyrins and PDIs has been extensively studied, especially by Wasielewski and Lindsey in the 1990s.[31,32,94,100,115] Figure 9 shows a donor–acceptor–donor (D–A–D) compound **7** containing a PDI and two porphyrin moieties reported by Wasielewski and co-workers in 1992.[31] The growth and decay of a PDI radical-anion absorption (observed at ca. 713 nm via transient absorption spectroscopy) indicates that photoexcitation of the porphyrin moieties at 585 nm results in the formation of a D^+–A^-–D charge-separated state with a rate constant of 1.1×10^{11} s^{-1} and that subsequent charge

recombination occurs with a rate constant of 9.1×10^9 s^{-1}. Further excitation of this molecule with much higher intensity irradiation at 580 nm can result in the formation of a D^+–A^{2-}–D^+ doubly charge-separated state, as demonstrated by the observation of a PDI dianion absorption at ca. 546 nm in transient absorption spectra, the rate constants for both charge-separation $(5.6 \times 10^9$ $s^{-1})$ and charge-recombination rates $(2.2 \times 10^8$ $s^{-1})$ being much lower than for the singly charge-separated state. Since the radical anion and dianion show quite different absorption behavior (see also Figure 7), the triad
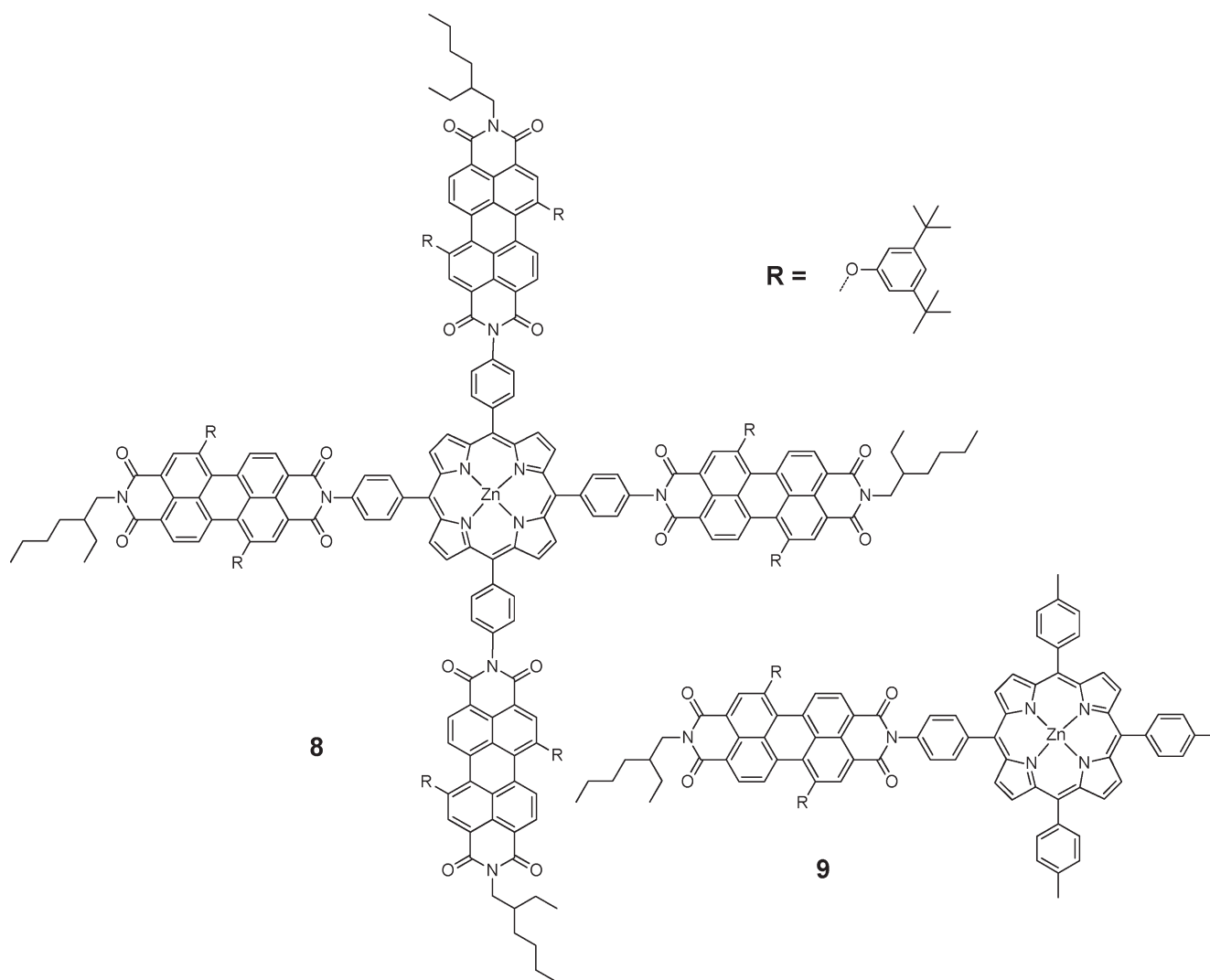
Figure 10. Chemical structures of tetrakis(PDI)-substituted zinc tetraphenylporphyrin and a model compound.
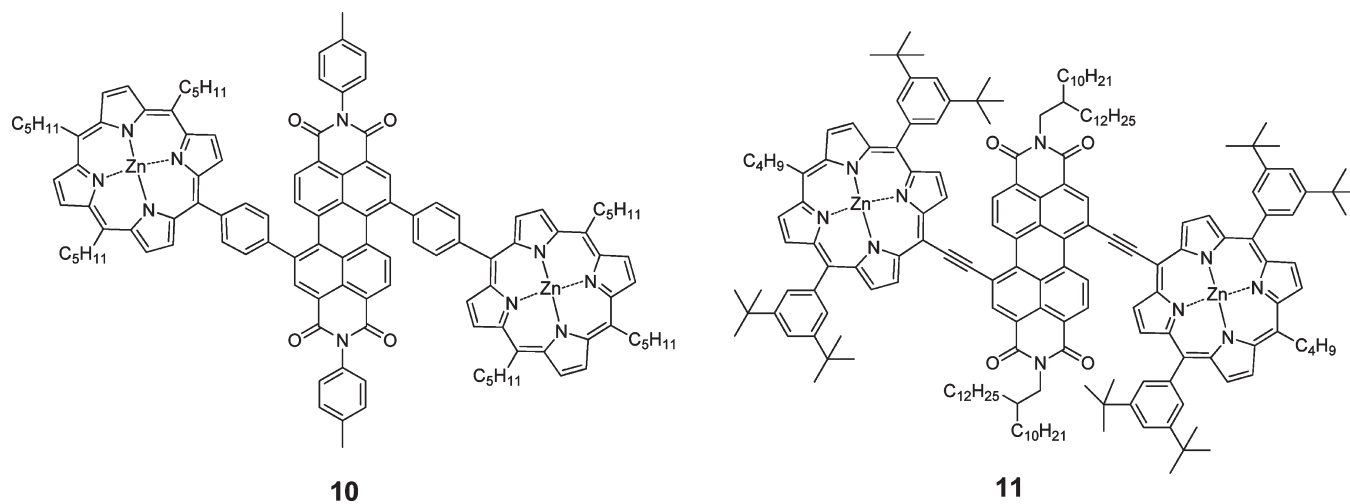
Figure 11. Chemical structures of two bis(porphyrin) PDI with conjugated linkers.

could serve as a light intensity-dependent optical switch; such processes could serve as models for biexcitonic states

that are being discussed in the context of photovoltaic systems.[31]

Figure 12. Chemical structures of PDI-based systems studied by transient absorption with substituents other than porphyrins.
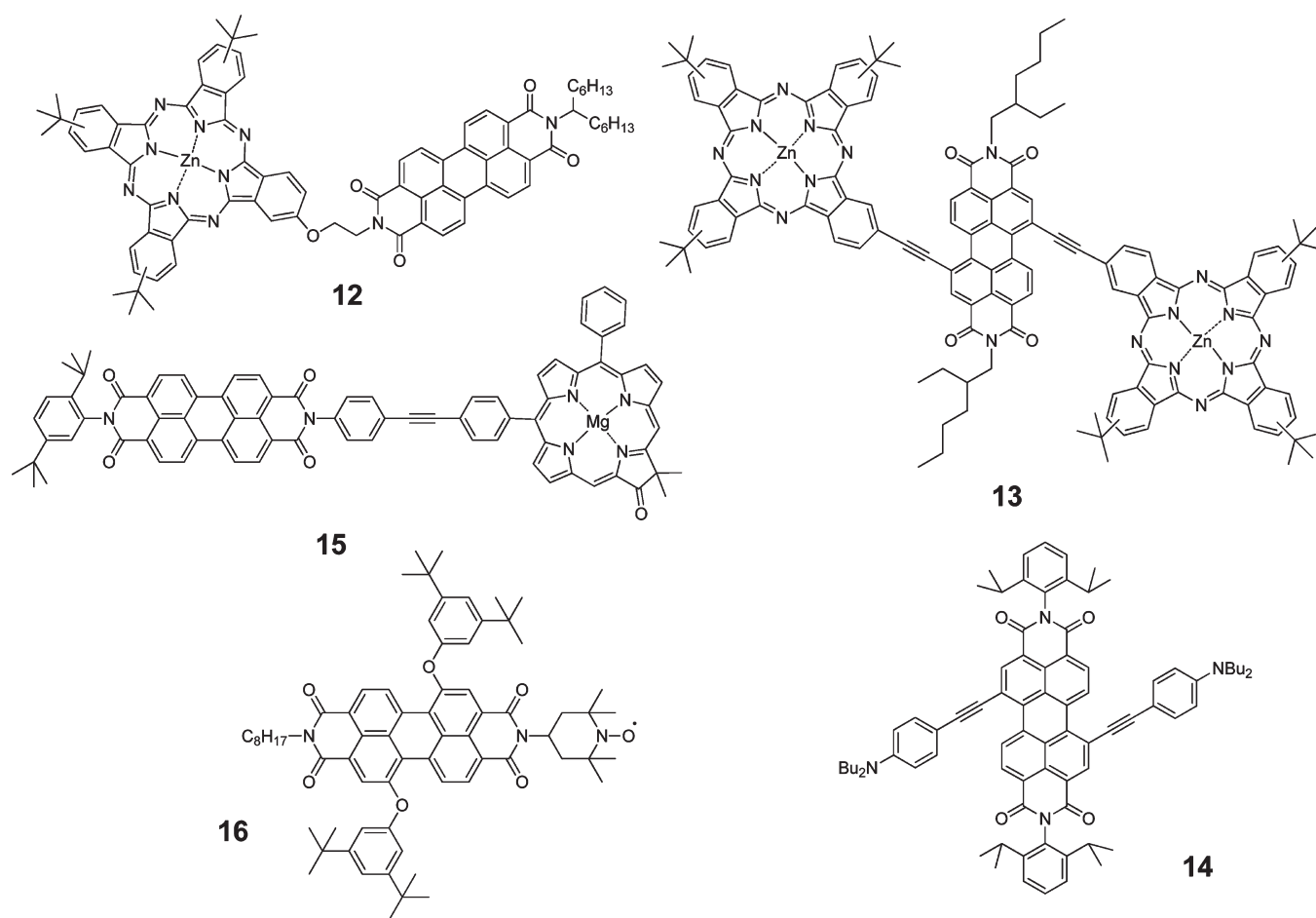
The tetrakis(PDI)-substituted zinc tetraphenylporphyrin shown in Figure 10 self-assembles in solution into nanoparticles with an average of 12 molecules in each nanoparticle.[100] Photoinduced ET within these particles occurs with near-unity efficiency with a rate constant of 3.1×10^{11} s^{-1}, while the resultant charge-separated state recombines with a rate constant of 1.4×10^{8} s^{-1}. The photoinduced charge-separation rate is ca. 4 times greater and charger recombination of the particles is ca. 1.4 times slower than those for **9**, the mono-PDI-functionalized zinc porphyrin model compound (also shown in Figure 10). The transient-absorption spectra of the photogenerated PDI anion in the nanoparticles are broader and lower in peak intensity (ca. 720 nm) than those for the model compound; it was suggested that this might be due to the delocalization of the negative charge from PDI^{-} onto the other PDI units that were within van der Waals distances in the nanoparticles.[100] It is worth noting that possible role of $(PDI)_n^{-}$ species in stabilizing the charge-separated state could potentially be explored for other applications such as OPVs and optical power limiting where charge-separated states with longer lifetimes can play a useful role.

Research on the photophysics of the porphyrin–PDI materials with conjugated linkers has also been conducted.[115,116] Electronic coupling between the porphyrins and PDI is not very strong in triad **10** as evidenced by its optical and redox properties, likely due to a substantial twist angle between the phenylene spacer and the PDI and/or porphyrin units. Both the photoinduced charge-separation and recombination rates in toluene

(with 1% pyridine) are quite fast (rate constants of 1.0×10^{11} s^{-1} and 1.3×10^{10} s^{-1}, respectively). UV–vis–NIR absorption spectra and transient absorption spectra suggest that the recently studied bay-ethynylene-linked porphyrin–PDI–porphyrin triad (**11**) shown in Figure 11[116] is characterized by considerably stronger donor–acceptor interaction than the weakly coupled species shown in Figures 9 and 10 or than triad **10**. A transient state, which was suggested to have significant charge-transfer character, was formed within 10 ps of photoexcitation (at a variety of vis.-NIR wavelengths) and had a lifetime of ca. 290 ps, the lifetime being slightly longer than that of the charge-separated state formed by triad **10** and **7**[31,115] but shorter than those in some other alkyne-bridged bis(donor) PDI systems reported in literature.[19,33]

Photoinduced processes in donor–PDI systems other than porphyrin-PDI conjugates have also been well studied. Photoexcitation of a dyad composed of a zinc phthalocyanine (ZnPc) and PDI (**12**, Figure 12)[35] afforded the triplet excited state (ZnPc–^{3}PDI*), whereas the photoexcitation of **12** in the presence of Mg^{2+} was reported to lead to the efficient (quantum yield of 72%) formation of a state with a rather long lifetime of up to 240 μs; this was considered by the authors to be a charge-separated state (ZnPc$^+$–PDI$^-$/Mg^{2+}) in which the PDI radical anion forms a complex with Mg^{2+} and which is lower in energy than the ZnPc–^{3}PDI* state. The absorption band attributed to the ZnPc$^+$–PDI$^-$/Mg^{2+} complex (λ_{max} = ca. 500 and 550 nm) is significantly shifted from that of an isolated PDI radical anion
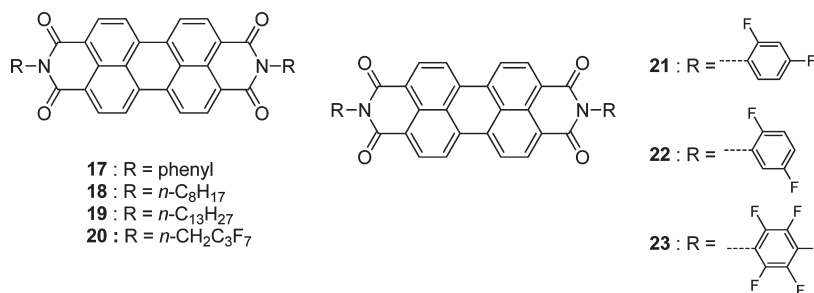
Figure 13. Some PDI derivatives used for OFET applications.

(λ_{max} = ca. 720 nm); there is, however, no direct evidence for the formation of the proposed complex.[35] Photoexcitation of a more strongly coupled Pc−PDI−Pc triad **13** (Figure 12) produces only a charge-separated state with lifetime of ca. 0.5 ns, with no evidence for formation of PDI triplets[19] (the triplet−triplet absorption spectrum of typical PDIs exhibits a peak at ca. 500 nm[12]) being seen in the transient absorption spectra. Another type of bis(donor)-PDI compound, **14**, with strong electronic coupling between the triphenylamine-based donors and the PDI moiety, also exhibits rapid (ca. 10 ps) photoinduced formation of a state that exhibits a PDI$^-$-like spectrum, indicating considerable charge-transfer character, and a ca. 2 ns lifetime; however, variation of the details of the structure of the amine donor group leads to wide variation in the excited-state lifetimes (82 ps to 2.1 ns).[33] Efficient photoinduced charge transfer also occurs in PDI−(Mg)oxochlorin (PDI−MgOx, **15**) with oxochlorin-to-PDI electron transfer occurring in high yield (>90%) in solution. The charge-separated state for **15** has a lifetime longer than 1 ns in both toluene and benzonitrile. The pathway for the generation of PDI$^-$−MgOx$^+$ from the excited PDI species involves both hole transfer and energy transfer to the oxochlorin, the latter process is then followed by ET from MgOx* to PDI. The overall yield of MgOx-to-PDI ET was found to be ca. 70% and 85% in toluene and benzonitrile respectively.[117,118] Very recently, the photoinduced charge transfer of dyad **16** (TEMPO-PDI)[119] was studied by Wasielewski and co-workers. It was found that efficient ET occurs in **16** to generate PDI radical anion on excitation of the PDI in THF with charge-separation and recombination rate constants of 8.3×10^{11} s^{-1} and 2.2×10^8 s^{-1}, respectively. However, intersystem crossing occurs with a rate constant of 2.2×10^{10} s^{-1}, generating TEMPO−^{3}PDI* following PDI excitation in toluene. The solvent-dependent quenching mechanisms of **16*** were attributed to the different free energies of the ET reaction of **16*** in different solvents (−0.81 eV in THF and −0.31 eV in toluene).[119,120]

In general, photoexcitation of weakly coupled donor-PDI systems generates relatively long-lived charge-separated states, with PDI radical anions and/or dianions showing strong absorption band peaks at ca. 720 nm and/or 550 nm, respectively.[12,31] Because PDIs without chemical modification at the bay positions exhibit high linear transparency in the NIR, these photogenerated ions could potentially be utilized for optical-limiting applications at wavelengths at which the radical anion absorbs strongly if appropriate molecular donors are chosen in building up the donor-PDI conjugates.[121−123] However, to our knowledge, there are no reports on using photogenerated PDI radical-ion absorption for optical-limiting applications with donor-PDI type materials or blends of PDI and donors, perhaps due to the challenge of obtaining long-lived charge-separated states (>1 ns) together

with sufficient ground-state absorption or two-photon absorption (2PA) in the same spectral range as that in which PDI anions absorb.

4. PDIS IN ORGANIC ELECTRONICS

4.1. OFETs. PDIs are attractive candidates for use as the active layer of n-channel field-effect transistors; their relatively exergonic electron affinities (using electrochemical data one can estimate a value of ca. −3.9 eV for simple N,N'-dilkakyl or diaryl PDIs without core substitution in the solid state)[5,10,18,124] suggest the possibility of facile electron injection and, therefore, potentially low threshold voltages; the ability for some examples to form highly ordered π-stacked structures suggests the possibility of high charge-carrier mobilities; and the range of structural modifications that can be made through imide and bay positions can be used to tune electronic and morphological properties. n-Channel field-effect transistors were fabricated using the related anhydride PTCDA (Figure 1) by Ostrick and co-workers in 1997: electron mobilities measured in bottom-contact devices were found to be ca. 10^{-4} cm^2 V^{-1} s^{-1} when the devices were operated in vacuum.[125] PDI-based transistors were first demonstrated by Horowitz and co-workers in 1996 using vacuum-deposited **17** (Figure 13) as the active material and gave electron mobilities of 10^{-5} cm^2 V^{-1} s^{-1}.[126] N,N'-Alkyl-substituted PDIs (**18** and **19** in Figure 13)[127,128] were also investigated as electron-transport materials in OFETs. Malenfant and co-workers reported that bottom-contact devices using films from vacuum-deposited **18** (substrate temperature kept at 50 °C) showed electron mobilities of 0.6 cm^2 V^{-1} s^{-1} with I_{on}/I_{off} > 10^5 in vacuum. However, these devices required very high gate voltages for operation, and the threshold voltage was very high (ca. 75 V). An electron mobility of 2.1 cm^2 V^{-1} s^{-1} with I_{on}/I_{off} = 4.2×10^5 was recently reported by Tatemichi and co-workers for devices based on **19**; the authors attributed the high electron mobilities to the improvement of the crystallinity of **19** in films after thermal annealing at 140 °C.[127] Recently, Oh and co-workers utilized the fluoroalkyl-substituted PDI **20** in vacuum-deposited OFETs. The electron mobilities of these devices were as high as 0.72 cm^2 V^{-1} s^{-1} in vacuum and 0.51 cm^2 V^{-1} s^{-1} in air. There was no obvious change in I_{on}/I_{off} (ca. 10^6) for transistors measured in vacuum and air.[6,106]

N,N'-Bis(pentafluorophenyl)-substituted PDI **23** and related compounds (**21** and **22**) developed by Chen and co-workers were demonstrated to be good, air-stable materials in n-channel OFETs.[129] The electron mobilities of OFETs based on **21**, **22**, and **23** were found to be 0.011, 0.026, and 0.042 cm^2 V^{-1} s^{-1}, respectively, in ambient atmosphere. These values were reduced by only 5−25% from those measured in vacuum. As discussed
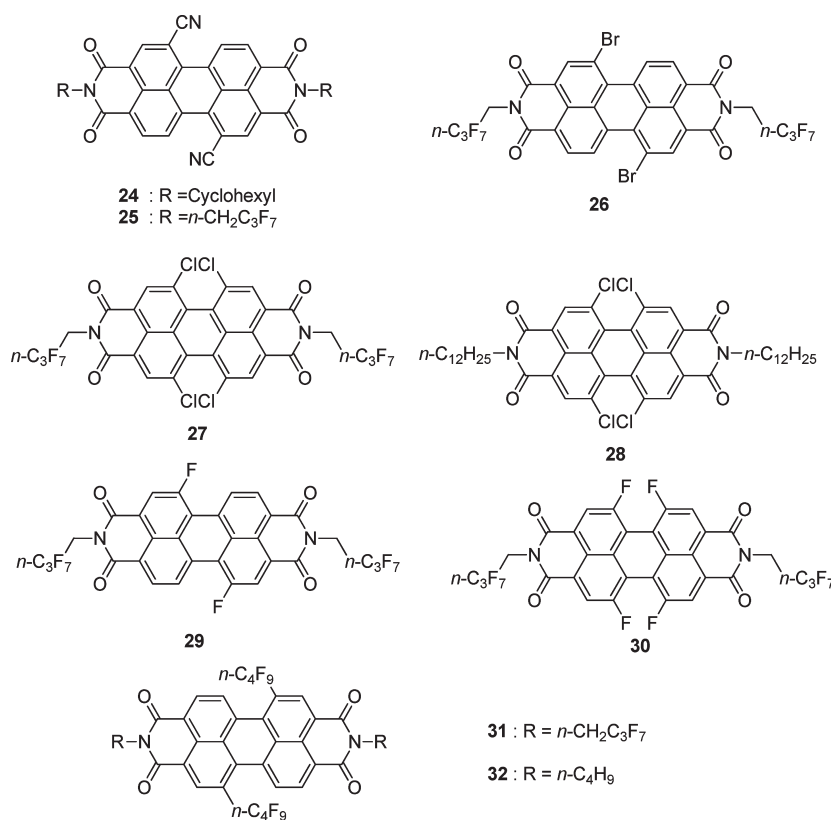
Figure 14. Bay-substituted PDI derivatives used as electron-transport materials.

above, the electrochemical properties, and therefore presumably the electron affinities, of these fluorinated-PDI-based materials are quite similar to their nonfluorinated counterparts (estimated EAs only ca. 0.1 eV more exergonic); the improved air stability of the OFETs has, therefore, been attributed to the better molecular packing of the fluorinated-PDIs in vacuum-deposited films, with fluorinated substituents effectively preventing the penetration of oxygen and water.[20] A similar explanation has also been applied to the air stability of devices based on **20**.

PDIs with substitutions in the bay positions have also been studied as active materials in n-channel OFETs. Dicyano-substituted perylene diimides **24** and **25** (Figure 14) developed by Jones and co-workers exhibit considerably more exergonic estimated electron affinities, as well as high solubility. The electron mobilities in top-contact devices were found to be 0.1 and 0.64 cm^2 V^{-1} s^{-1} and I_{on}/I_{off} values of ca. 10^5 were found using vacuum-deposited films from **24** and **25**, respectively, in ambient atmosphere. Top-contact devices fabricated from drop-cast films were also found to be air stable and exhibited mobilities up to 10^{-3} cm^2 V^{-1} s^{-1} for these devices.[10,18] Bay-halogenated PDIs **26** and **27** were recently investigated by the same group. It was found that devices of these materials operated in ambient atmosphere showed similar performance as those operated in vacuum, although the electron mobilities (ca. 10^{-4}–10^{-5} cm^2 V^{-1} s^{-1}) were much lower than those of **24** and **25** in similar device geometries. One possible explanation for the poor device performance is the nonplanarity of PDI cores and consequently poor π–π stacking in these materials.[6,105] However, another tetrachloro-substituted perylene diimide (**28**) was found to have a charge-carrier mobility of 0.14 cm^2 V^{-1} s^{-1} using the pulse-radiolysis time-resolved microwave conductivity technique (PR-TRMC),[130]

which suggests that these types of materials might still be good candidates for transistor applications if the film morphology could be well controlled.[131] In order to reduce the steric effects from bay halogen substituents, materials with fluorine in the bay positions were also examined; the electron mobilities of vacuum-deposited films of **29** and **30** were found to be 0.34 and 0.031 cm^2 V^{-1} s^{-1} with I_{on}/I_{off} >10^5 in ambient atmosphere, with the higher mobility of the **23**-based device being attributed to a smaller distortion of the PDI core from planrity.[57,58] Recently, PDIs with perfluoralkyl chains in the bay positions, **31** and **32** (Figure 14), were developed by Li and co-workers; **32** showed electron mobilities up to 0.052 cm^2 V^{-1} s^{-1} with I_{on}/I_{off} = 8×10^6 under ambient conditions, with these values being little different from those measured in vacuum. The electron mobility of **31** was only 0.005 cm^2 V^{-1} s^{-1} with I_{on}/I_{off} = 4×10^3. However, the turn-on voltage for devices from **31** was 4.7 V, ca. 10 times lower than that for devices from **32**.[132]

Recently, wet-processing of high-mobility PDIs has been investigated; some of the materials examined are shown in Figure 15. A columnar liquid-crystalline (LC) material **33** was found to exhibit charge mobility of 0.1 cm^2 V^{-1} s^{-1} in the LC phase (ca. 220 °C) and a charge-carrier mobility as high as 0.2 cm^2 V^{-1} s^{-1} in the crystalline phase using PR-TRMC.[133] In 2005, a room-temperature columnar LC material **34** was reported to exhibit electron mobilities as high as 1.3 cm^2 V^{-1} s^{-1} under ambient atmosphere using the steady-state space-charge-limited current technique; this electron mobility is higher than that of amorphous silicon. However, electron mobilities of the material measured using other techniques were low, presumably in part reflecting difficulties in achieving the required alignment of the
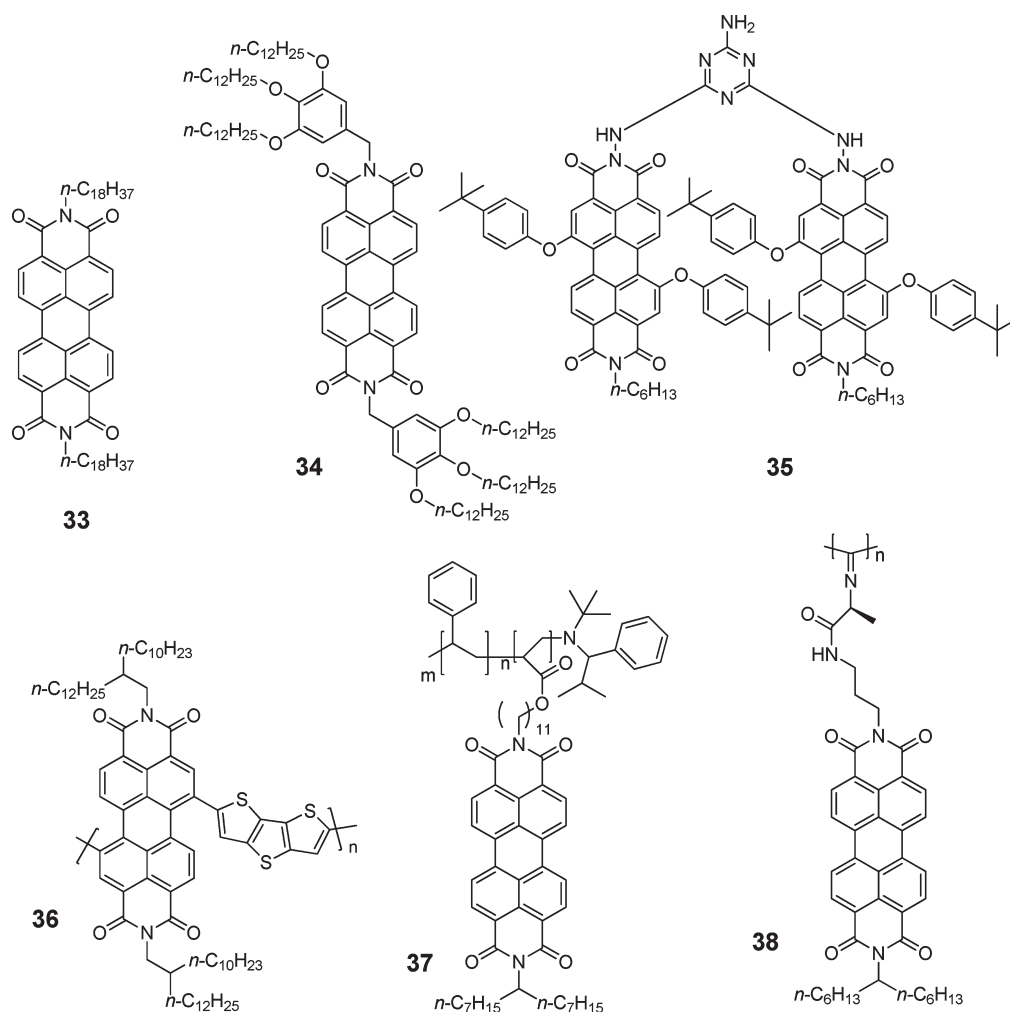
Figure 15. Some solution-processable PDI-based electron-transport materials.

**Table 3. Performance of Bilayer Solar Cells Containing PDI-Based Acceptors**

devices	V_{oc}/V	J_{sc}/mAcm^{-2}	FF	PCE/%	ref
ITO/CuPc/**3**/Ag	0.45	2.3	0.65	1.0	142
ITO/DMP/H$_2$Pc/Au^a	0.54	0.94	0.48	0.29	144
ITO/DMP/ClAlPc/Ag^a	0.31	1.71	0.41	1.21	145
ITO/CuPc/**3**/BCP/Ag	N.A.	N.A.	0.54	2.4	143
ITO/PEDOT-PSS/pentacene/**13**/BCP/Ag	0.40	5.0	0.64	1.6	148
ITO/**3**/MEH-PPV/Au	0.56	2.4	0.29	0.40	147
ITO/**3**/PPAV-HH-PPV/Au	0.48	2.5	0.28	0.33	147

^{a} DMP is Pigment Red 179, N,N'-dimethyl PDI, which is shown in Figure 2.

π-stacked columns with respect to the substrate.[9,134] Field-effect transistors using highly ordered Langmuir−Blodgett films formed by compound **35** have been fabricated and studied by Wang and co-workers; within the top-contact devices, the molecules kept the desired face−face π-stacking configuration, and the electron mobilities were found to be as high as 0.05 cm^2 V^{-1} s^{-1} with I_{on}/I_{off} > 10^3.[135] PDI-based D−A conjugated polymers such as **36** have also been investigated as electron-transport material in OFETs; spin-coated films of **37** were found to exhibit electron mobilities as high as 0.013 cm^2 V^{-1} s^{-1} with I_{on}/I_{off} > 10^4 in top-contact OFETs under nitrogen. The electron

mobility of this material is among the highest value reported in conjugated polymers to date.[16] The concept of using rylene diimide-donor polymers as electron-transport materials has been further developed by Facchetti and co-workers, and an OFET electron mobility approaching 1 cm^2 V^{-1} s^{-1} has recently been reported for a naphthalene diimide-bithiophene polymer.[88,136] Side chain polymers **37** and **38** with PDI pendants have also been investigated as electron-transport materials in OFET devices; electron mobilities of 1.2 × 10^{-3} cm^2 V^{-1} s^{-1} with I_{on}/I_{off} > 10^4 were reported for polymer **37** when spin-cast films were thermally annealed at 210 °C for 60 min in
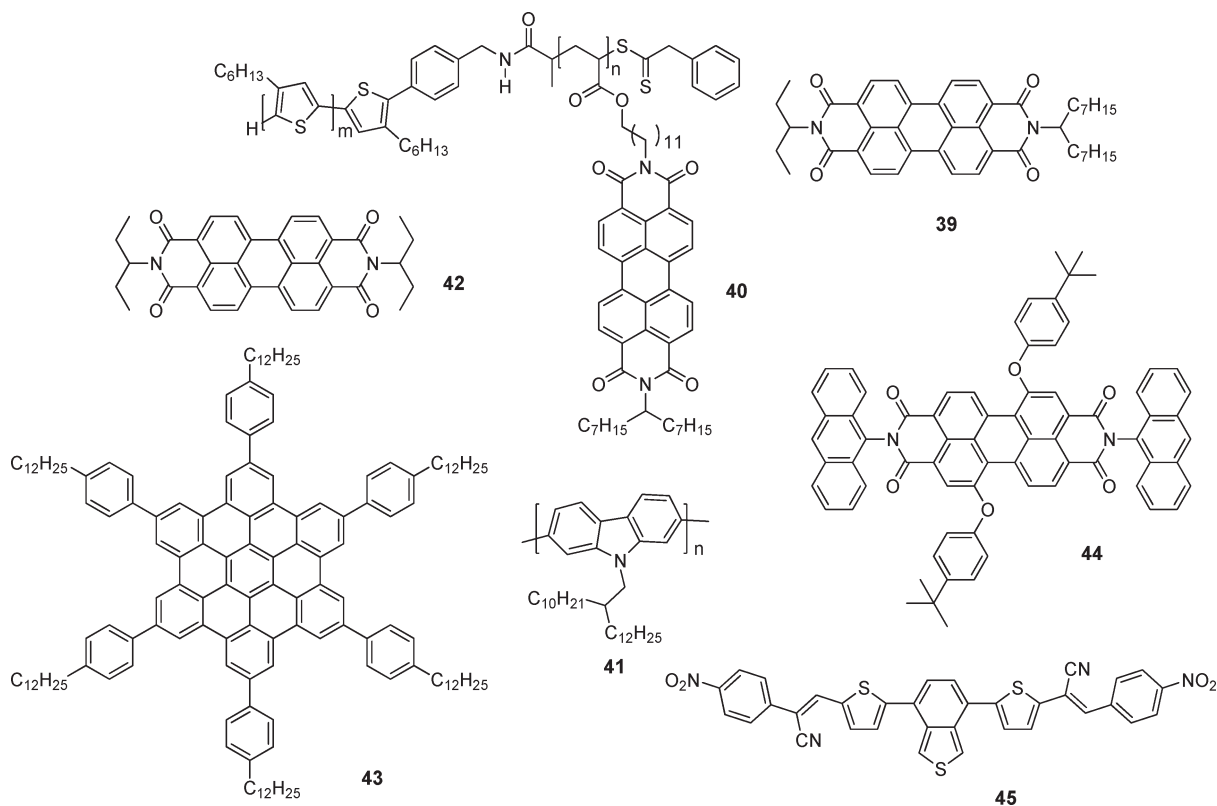
Figure 16. Some materials used in solution processable solar cells incorporating PDI derivatives.

bottom-contact OFETs. Similar device performance was achieved for **38** at 360 K using top contacts.[52,137]

4.2. Solar Cells. PDIs are attractive as potential electron-transport materials for use in organic solar cells due to the high electron mobilities possible (see section 4.1) and their exergonic electron affinities (ca. −3.9 eV for simple PDIs[98]), which are appropriate for use in combination with many commonly used donor materials and which are similar to those of the fullerenes widely used as acceptors in bulk-heterojunction solar cells.[138−141] Moreover, the functionalization chemistry of PDIs is more easily accomplished than that of fullerene-based acceptors,[5,26,45] while their strong and tunable visible absorptions offers the possibility of use as light-absorbing materials rather than purely transport materials.[26,45] Indeed, the first bilayer organic solar cells, which were reported by Tang in 1986, utilized a benzoimidazole PDI derivative (**3**, Figure 5) as the acceptor and copper phthalocyanine (CuPc) as donor (ITO/CuPc/**3**/Ag). The power conversion efficiencies (PCEs) of the devices approached 1%.[142] Subsequently, Pc and PDI derivatives have been commonly used in thin-film organic solar cells.[143−145] Recently, following Tang's basic device structure, external PCEs of 2.4% have been demonstrated within a thin-film solar cell in which the incident photons could pass through the light-absorbing organic layers multiple times to avoid the mismatching of exciton diffusion length and optical absorption length.[143] In these devices, the incorporation of an exciton-blocking layer (of bathocuproine, BCP)[143] between the organic layers and the metal cathode is reported to play an essential role in preventing damage during the cathode deposition[146] and in eliminating exciton quenching at the organic/metal interface.[104] Inverted bilayer solar cells with a structure consisting a spin-cast hole-transporting conjugated polymer, such as (poly(2-methoxy-5-(2′-ethylhexyloxy)-1,4-phenylenevinylene)

(MEH-PPV) and (poly(phenylimino-1,4-phenylene-1,2-ethenylene-2,5-dihexyloxy-1,4-phenylene-1, 2-ethenylene-1,4-phenylene) (PPAV-HH-PPV), on top of an insoluble **3** electron-transport layer show PCEs of ca. 0.4%.[147] Furthermore, ITO and Au electrodes were modified with indium and PEDOT:PSS, respectively, resulting in significantly improved solar-cell efficiencies Moreover, the utilization of the wide range of absorption by exciton confinement could remarkably improve the PCEs of these cells up to 2%.[147] Bilayer organic solar cells containing vacuum-deposited PDI-based acceptors and organic small molecular donors such as pentacene[148] and rubrene[129] can afford PCEs up to 2% after optimization of device structures. Some of these achievements are summarized in Table 3.

More limited progress has been achieved with wet-processed bulk-heterojunction solar cells incorporating PDIs than with PDI-based vacuum-deposited layered solar cells. While the causes for the low PCEs achieved to date are not clear, it has been suggested that formation of micrometer-sized (or even larger) PDI-based aggregates in the blend films could lead to incomplete exciton dissociation.[26] On the other hand, transient-absorption studies of blends of poly(thiophene)s such as poly(3-hexylthiophene) (P3HT) and a PDI small molecule (**34**, as shown in Figure 15) indicates greater yields of free carriers than in analogous blends with PCBM as the acceptor, suggesting exciton dissociation can, at least in some cases be reasonably efficient,[114] and that perhaps that collection of these charges is the limiting factor. Solar cells composed of blends of PDIs and P3HT exhibit low PCEs (typically below 0.05%). Recently, by using an asymmetric PDI derivative (**39**), PCEs as high as 0.37% have been demonstrated for a P3HT:PDI blend; device performance could be further enhanced in the presence of the compatibilizer (**40** as shown in Figure 16), and optimized solar
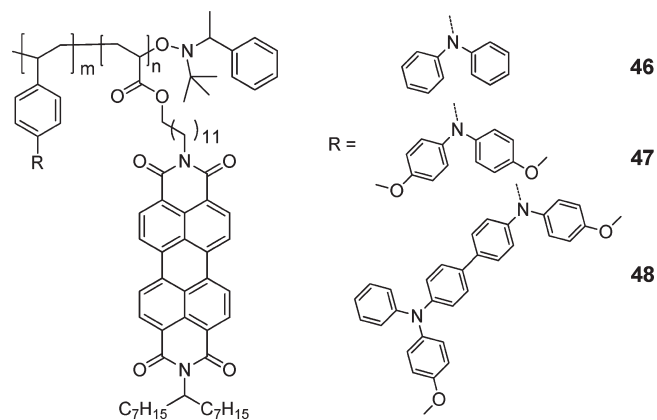
Figure 17. PDI-based diblock copolymers for OPV applications.

Figure 18. Some PDI-based "double-cable" polycarbazole copolymers used for OPVs.

cells afforded a PCE of 0.55% and were shown to contain smaller PDI domains in the active layer.[149] Müllen and co-workers found that efficiencies of such devices could be greatly improved when P3HT was replaced with a poly(2,7-carbazole)-based donor (**41**, as shown in Figure 16).[150] The best photovoltaic device exhibits an external quantum efficiency (EQE) of 16% when irradiated at 490 nm, with overall PCEs of ca. 0.6% under AM 1.5 irradiation; scanning electron microscopy (SEM) of **41:42** blend films demonstrated the formation of more favorable phase separation (with smaller domains) than in P3HT/PDI blends.[150] Although these are among the best reported PCE and EQE values for solar cells using polymer/PDI blends, they are still much lower than those from devices fabricated using polymer/PCBM blends. Blends of columnar discotic LC donor (**43**, Figure 16) with **42** exhibit vertically segregated **43** and **42** domains in thin-films with large interfacial surface areas. Devices using a such blend exhibited an EQE up to 34% when irradiated at ca. 490 nm and an overall PCE ca. 2% under AM 1.5 irradiation.[25] Very recently, solar cells using a blend of **44** and a small-molecular donor (**45**, Figure 16) gave overall PCEs approaching 3% under AM 1.5 irradiation.[151] Both donor and acceptor materials contribute to the photocurrent in this device, contributing to a high short-circuit current density (J_{SC}, 6.6 mAcm^{-2}). Another factor contributing to the device performance may be due to the relatively balanced charge transport in the devices (hole and electron mobilities of ca. 1.0×10^{-4} cm^2 V^{-1} s^{-1} and 4.6×10^{-4} cm^2 V^{-1} s^{-1}, respectively). The charge-carrier mobilities for these high-efficiency solar cells[151] are actually quite close to those seen in P3HT:PCBM blends.[152]

One of recent promising approaches for photovoltaics is to use self-organizing or supramolecular materials to control the thin-film nanomorphology of the photoactive layer in devices.[153] The self-assembly of a block-copolymer (BCP) in which a block contains an electron donor and another block contains an electron acceptor can in principle give microphase separation to produce a highly regular nanometer-scale structure spontaneously during film preparation, which would be desirable for cost-effect device fabrications.[153] Thelakkat and co-workers reported such donor–acceptor diblock copolymers (Figure 17) with PDIs and triarylamines as electron-transport and hole-transport moieties, respectively, and were able to achieve spontaneous microphase separation to give desirable domain sizes (ca. 10 nm). Use of the copolymers led to an increase in the device efficiencies by an order-of-magnitude compared with those using a physical blend films of two homopolymers. Solar cells using polymer **48** show the best PCEs of 0.3%; favorable nanoscale phase separation in the bulk films being observed using
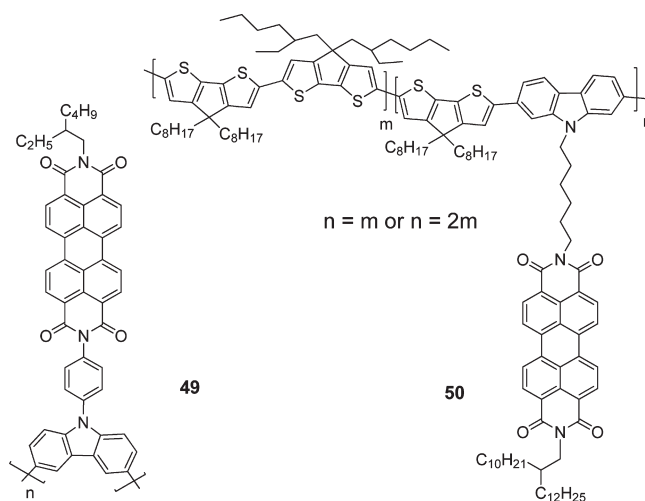
transmission electron microscopy.[17,49,51,52] Periodic nanometer-scale morphology could also successfully be accomplished using P3HT-block-PDI copolymers (**40** in Figure 16 and materials with similar chemical structures); using these materials as the photoactive layers in OPV cells has given PCEs of over 0.5%.[50,154] The state-of-the-art for this approach using block copolymers has some attractive advantageous oversimple polymer blends, including the easy control of phase-separation on length scales matched with exciton diffusion lengths and construction of an all-in-one material with various functional components for further performance enhancement, such as cross-linking groups for post-treatments and dyes that can improve solar light harvesting. However, the overall PCEs of the solar cells with the current diblock-copolymers are still far from satisfactory (<1%) for realistic applications.

Another group of PDI-based side-chain polymers are D–A-type "double-cable" copolymers with electron-donating conjugated backbones and PDIs as pendant acceptors. The conjugated polymeric architecture could potentially enhance π–π stacking interaction[30,91,155,156] between the PDI pendants, which, in principle, could stabilize the charge-separated states as well as facilitate charge carrier migration.[100] Moreover, because of their homogeneous molecular distribution and constant distance between the donor and acceptor building blocks (in contrast to simple donor/acceptor material blends in solar cells), "double-cable" polymers of such type might help overcome the phase-separation issues commonly encountered for physical blends and maximize the donor–acceptor interaction in the solid state for more efficient photoinduced charge separation. This could potentially benefit the preparation of high-quality films due to better control of film morphology. Solution-processed solar cells have been fabricated using these materials, as shown in Figure 18, as the active layers. For example, the PDI-grafted polycarbazole (polymer **49**) gave nearly 0.1% power conversion efficiency under simulated AM 1.5 (100 mW/cm^2) in single-polymer devices.[156] Solar cells with polymer **50** in blends with PCBM show enhanced performance compared to devices using the blend of PCBM and the polymer without PDI pendants. Moreover, it was also found that device performance was enhanced as more PDI moieties were incorporated into the copolymers.[155]
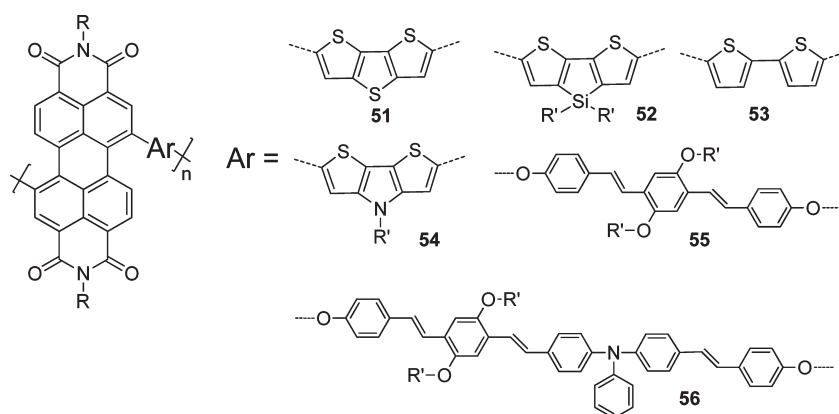
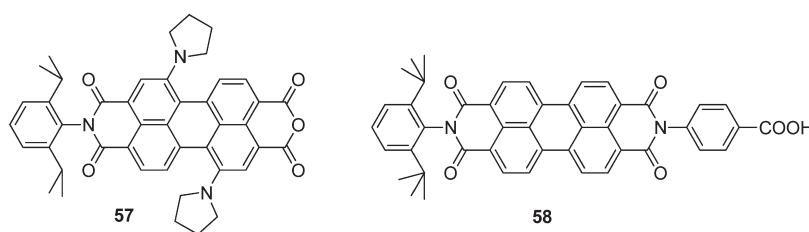**Figure 19.** PDI-based main-chain polymers linked through the bay positions and used in OPV studies.

Figure 20. Two PDI materials used as photosensitizers for dye-sensitized solar cells.

Recently PDI-donor-based conjugated polymers connected at the PDI 1,6(7)-bay positions have also been used in OPV cells in different research groups.[16,27,68,157,158] Polymers (Figure 19) have been synthesized in which PDIs are bridged by a variety of electron donor moieties including dithienothiophene,[16,27] dithienopyrrole,[68,87] bithiophene,[88] oligo(phenylenevinylene),[157] dithienosilole,[88] and triarylamine donors[157] through the bay positions. These generally showed good solubility and dramatically fluorescence quenching. Additionally, the electron mobilities of these kinds of polymers can be as high as 0.01 cm^2 V^{-1} s^{-1} as discussed above in the context of OFETs. OPV devices using these types of polymers in blends with appropriate polythiophene-based donor polymers or other donor—acceptor type polymers exhibit PCE as high as 1.5%; these are among the best devices using polymer—polymer blends.[16,27,89] One limitation is that, despite their broad absorption spectra, these materials contribute little to the light-harvesting in solar cells; for example, an EQE vs wavelength plot for a photovoltaic device based on a dithienothiophene-PDI polymer(**51**) /polythiophene blend is close to the absorption spectrum of the polythiophene itself, with little contribution from the lower energy absorptions of the PDI-based materials. Transient absorption spectra indicate that the dithienothiophene-PDI exciton (which appears to have significant charge-transfer character) has a lifetime of only several hundred picoseconds in solution, suggesting that in the blends only a limited number of DTT-PDI excitons may be able to diffuse to the interface with polythiophenes to undergo charge dissociation.[85]

Recently, PDI-based light-harvesting materials functionalized with groups such as carboxylic acid or anhydride (Figure 20) have also been used in dye-sensitized solar cells (Grätzel cells)[159] in combination with different bulk inorganic semiconductors.[160,161] The best reported DSSCs to date that utilize PDI-based dyes (**57**) exhibit PCEs of over 2.5% with a fill factor of 0.63.[161]

4. CONCLUSION

The organic chemistry of PDIs has been developed so that a wide range of substituents can be introduced in the imide or bay positions. Variation of the substituents at the imide position show only limited effects on the molecular-level optical and redox properties of PDIs; accordingly, imide substitution can be used to tune solubility, aggregation, and molecular packing in the solid state largely independently of the molecular electronic properties. On the other hand, the spectroscopic and redox properties can be significantly modified by introducing functional groups at the bay (or other perylene core) positions of PDIs.

The electron-accepting properties of PDIs have been extensively exploited in studied of photoinduced electron transfer and in organic electronics. PDIs are among the best materials examined to date for use in n-channel OFETs; high mobilities arising from efficient π stacking and operation in air have been demonstrated. To date, the best performance has been obtained in vacuum-deposited devices; the relatively modest mobilities found in solution-processed PDI devices limits their potential application in OFETs.

Vacuum-deposited bilayer solar cells incorporating PDI-based acceptors dyes give promising performance, suggesting that PDIs could potentially be used in highly efficient solution-processed bulk-heterojunction cells, although to date the performance of solution-processed devices has been rather poor. In our view, the causes for the poor performance of PDI bulk-heterojunction cells are not well understood. In some cases inefficient exciton dissociation due to unsuitable morphologies has been suggested to play a role, yet in other cases efficient charge generation is seen in transient absorption measurements. The strongly anisotropic electron mobilities expected for π-stacked PDIs may mean that obtaining efficient charge collection is more challenging than in analogous devices using more-or-less isotropic transport materials

based on fullerenes if π-stacks are inappropriately oriented with PDI domains. More studies aimed at developing a detailed understanding of the parameters affecting the photoinduced charge separation and the charge-carrier migration in solution-processed donor/PDI blends or in D—A type block copolymers would be valuable. Donor—acceptor diblock or multiblock copolymers are of particular promise given their ability to self-assemble into phase-separated structures with appropriate length scales; however, further efforts are required to obtain materials with better performance than those examined to date, i.e., with appropriately offset donor and acceptor energy levels, correct orientation of PDIs with the acceptor domains to enable efficient charge collection, and good coverage of the solar spectrum.

■ AUTHOR INFORMATION

Corresponding Author

*E-mail: seth.marder@chemistry.gatech.edu.

■ ACKNOWLEDGMENT

■ REFERENCES

(1) Herbst, W.; Hunger, K. *Industrial Organic Pigments*, 2nd completely revised ed.; Wiley-VCH: Weinheim, 1997.

(2) Kardos, M. German Patent, DE 276357, 1913.

(3) Kardos, M. German Patent, DE 276956, 1913.

(4) Kazmaier, P. M.; Hoffmann, R. *J. Am. Chem. Soc.* **1994**, *116*, 9684–9691.

(5) Würthner, F. *Chem. Commun.* **2004**, 1564–1579.

(6) Bao, Z.; Locklin, J. *Organic Field-Effect Transistors*; CRC Press: Boca Raton, FL, 2006.

(7) Serin, J. M.; Brousmiche, D. W.; Fréchet, J. M. J. *Chem. Commun.* **2002**, 2605–2607.

(8) Gronheid, R.; Hofkens, J.; Kohn, F.; Weil, T.; Reuther, E.; Müllen, K.; Schryver, F. C. D. *J. Am. Chem. Soc.* **2002**, *124*, 2418–2419.

(9) An, Z.; Yu, J.; Jones, S. C.; Barlow, S.; Yoo, S.; Domercq, B.; Prins, P.; Siebbeles, L. D. A.; Kippelen, B.; Marder, S. R. *Adv. Mater.* **2005**, *17*, 2580–2583.

(10) Jones, B. A.; Facchetti, A.; Wasielewski, M. R.; Marks, T. J. *J. Am. Chem. Soc.* **2007**, *129*, 15259–15278.

(11) Sadrai, M.; Bird, G. R. *Opt. Commun.* **1984**, *51*, 62–64.

(12) Ford, W. E.; Kamat, P. V. *J. Phys. Chem.* **1987**, *91*, 6373–6380.

(13) Seybold, G.; Wagenblast, G. *Dyes Pigm.* **1989**, *11*, 303–317.

(14) Weil, T.; Wiesler, U. M.; Herrmann, A.; Bauer, R.; Hofkens, J.; Schryver, F. C. D.; Müllen, K. *J. Am. Chem. Soc.* **2001**, *123*, 8101–8108.

(15) Ahrens, M. J.; Fuller, M. J.; Wasielewski, M. R. *Chem. Mater.* **2003**, *15*, 2684–2686.

(16) Zhan, X.; Tan, Z. A.; Domercq, B.; An, Z.; Zhang, X.; Barlow, S.; Li, Y.; Zhu, D.; Kippelen, B.; Marder, S. R. *J. Am. Chem. Soc.* **2007**, *129*, 7246–7247.

(17) Lindner, S. M.; Kaufmann, N.; Thelakkat, M. *Org. Electr.* **2007**, *8*, 69–75.

(18) Jones, B. A.; Ahrens, M. J.; Yoon, M.-H.; Facchetti, A.; Marks, T. J.; Wasielewski, M. R. *Angew. Chem., Int. Ed.* **2004**, *43*, 6363–6366.

(19) Jiménez, A. J.; Spänig, F.; Rodríguez-Morgade, M. S.; Cai, S.; Fukuzumi, S.; Guldi, D. M.; Torres, T. *Org. Lett.* **2007**, *9*, 2481–2484.

(20) Chen, H. Z.; Ling, M. M.; Mo, X.; Shi, M. M.; Wang, M.; Bao, Z. *Chem. Mater.* **2007**, *19*, 816–824.

(21) Jung, B. J.; Tremblay, N. J.; Yeh, M.-L.; Katz, H. E. *Chem. Mater.* **2011**, *23*, 568.

(22) Zhan, X. W.; Facchetti, A.; Barlow, S.; Marks, T. J.; Ratner, M. A.; Wasielewski, M. R.; Marder, S. R. *Adv. Mater.* **2011**, *23*, 268–284.

(23) Gvishi, R.; Reisfeld, R.; Burshtein, Z. *Chem. Phys. Lett.* **1993**, *213*, 338–344.

(24) Law, K. Y. *Chem. Rev.* **1993**, *93*, 449–486.

(25) Schmidt-Mende, L.; Fechtenkötter, A.; Müllen, K.; Moons, E.; Friend, R. H.; MacKenzie, J. D. *Science* **2001**, *293*, 1119–1122.

(26) Wang, H.; Peng, B.; Wei, W. *Progress Chem.* **2008**, *20*, 1751–1760.

(27) Tan, Z. A.; Zhou, E.; Zhan, X.; Wang, X.; Li, Y.; Barlow, S.; Marder, S. R. *Appl. Phys. Lett.* **2008**, *93*, 073309.

(28) Anthony, J. E. *Chem. Mater.* **2011**, *23*, 583–590.

(29) Belfield, K. D.; Bondar, M. V.; Hernandez, F. E.; Przhonska, F. E. *J. Phys. Chem. C* **2008**, *112*, 5618–5622.

(30) Huang, C. Ph.D Thesis, Georgia Institute of Technology, 2010.

(31) O'Neil, M. P.; Niemczyk, M. P.; Svec, W. A.; Gosztola, D.; Gaines, L. G.; Wasielewski, M. R. *Science* **1992**, *257*, 63–65.

(32) Prathapan, S.; Yang, S. I.; Seth, J.; Miller, M. A.; Bocian, D. F.; Holten, D.; Lindsey, J. S. *J. Phys. Chem. B* **2001**, *105*, 8237–8248.

(33) An, Z. S.; Odom, S. A.; Kelley, R. F.; Huang, C.; Zhang, X.; Barlow, S.; Padilha, L. A.; Fu, J.; Webster, S.; Hagan, D. J.; Van Stryland, E. W.; Wasielewski, M. R.; Marder, S. R. *J. Phys. Chem. A* **2009**, *113*, 5585–5593.

(34) Shoaee, S. A., Z.; Zhang, X.; Barlow, S.; Marder, S. R.; Duffy, W.; Heeney, M.; McCulloch, I.; Durrant, J. R. *Chem. Commun.* **2009**, 5445–5447.

(35) Fukuzumi, S.; Ohkubo, K.; Ortiz, J.; Gutierrez, A. M.; Fernandez-Lazaro, F.; Sastre-Santos, A. *Chem. Commun.* **2005**, 3814–3816.

(36) Maki, T.; Hashimoto, H. *Kogyo Kagaku Zasshi* **1951**, *54*, 544–547.

(37) Maki, T.; Hashimoto, H. *Bull. Chem. Soc. Jpn.* **1952**, *25*, 411–413.

(38) Langhals, H. *Heterocycles* **1995**, *40*, 477–500.

(39) Wescott, L. D.; Mattern, D. L. *J. Org. Chem.* **2003**, *68*, 10058–10066.

(40) Rademacher, A.; Märkle, S.; Langhals, H. *Chem. Ber.* **1982**, *115*, 2927–2934.

(41) Huang, Y.; Yan, Y.; Smarsly, B. M.; Wei, Z.; Faul, C. F. J. *J. Mater. Chem.* **2009**, *19*, 2356–2360.

(42) Backes, C.; Schmidt, C.; Hauke, F.; Böttcher, C.; Hirsch, A. *J. Am. Chem. Soc.* **2009**, *131*, 2172–2173.

(43) Heek, T.; Fasting, C.; Rest, C.; Zhang, X.; Würthner, F.; Haag, R. *Chem. Commun.* **2010**, *46*, 188–1886.

(44) Liu, Y.; Wang, K.-R.; Guo, D.-S.; Jiang, B.-P. *Adv. Funct. Mater.* **2009**, *19*, 2230–2235.

(45) Nagao, Y. *Prog. Org. Chem.* **1997**, *31*, 43–49.

(46) Maki, T.; Hashimoto, H. *Bull. Chem. Soc. Jpn.* **1954**, *27*, 602–605.

(47) Wicklein, A.; Kohn, P.; Ghazaryan, L.; Thurn-Albrecht, T.; Thelakkat, M. *Chem. Commun.* **2010**, *46*, 2328–2230.

(48) Iverson, I. K.; Tam-Chang, S.-W. *J. Am. Chem. Soc.* **1999**, *121*, 5801–5802.

(49) Sommer, M.; Lindner, S. M.; M, T. *Adv. Funct. Mater.* **2007**, *17*, 1493–1500.

(50) Sommer, M.; Lang, A. S.; Thelakkat, M. *Angew. Chem., Int. Ed.* **2008**, *47*, 7901–7904.

(51) Lindner, S. M.; Huttner, S.; Chiche, A.; Thelakkat, M.; G. Krausch, A. *Angew. Chem., Int. Ed.* **2006**, *45*, 3364–3368.

(52) Hüttner, S.; Sommer, M.; Thelakkat, M. *Appl. Phys. Lett.* **2008**, *92*, 093302.

(53) Würthner, F.; Sautter, A.; Schilling, J. *J. Org. Chem.* **2002**, *67*, 3037–3044.

(54) Rogovik, V.; Gutnik, L. *Zh. Org. Khim.* **1988**, *24*, 635–639.

(55) Seybold, G.; Wagenblast, G. *Dyes Pigm.* **1989**, *11*, 303–317.

(56) Iden, R.; Seybold, G. *Ger. Pat. Appl.*, 1985; Vol. DE 3434059 A1.

(57) Schmidt, R.; Ling, M. M.; Oh, J. H.; Winkler, M.; Könemann, M.; Bao, Z.; Würthner, F. *Adv. Mater.* **2007**, 3692–3695.

(58) Würthner, F.; Osswald, P.; Schmidt, R.; Kaiser, T. E.; Mansikkama, H.; Könemann, M. *Org. Lett.* **2006**, *8*, 3765–3768.

(59) Böhm, A.; Arms, H.; Henning, G.; Blaschka, P. *Ger. Pat. Appl.*, 1997; Vol. DE 19547209 A1.

(60) Würthner, F.; Stepanenko, V.; Chen, Z.; Saha-Moller, C. R.; Kocher, N.; Stalke, D. *J. Org. Chem.* **2004**, *69*, 7933–7939.

(61) Schmidt, R.; Oh, J. H.; Sun, Y.-S.; Deppisch, M.; Krause, A.-M.; Radacki, K.; Braunschweig, H.; Könemann, M.; Erk, P.; Bao, Z.; Würthner, F. *J. Am. Chem. Soc.* **2009**, *131*, 6215–6216.

(62) Hill, Z. B.; Rodovsky, D. B.; Leger, J. M.; Bartholomew, G. P. *Chem. Commun.* **2008**, *45*, 6594–6596.

(63) Rajasingh, P.; Cohen, R.; Shirman, E.; Shimon, L. J. W.; Rybtchinsk, B. *J. Org. Chem.* **2007**, *72*, 5973–5979.

(64) Ahrens, M. J.; Fuller, M. J.; Wasielewski, M. R. *Chem. Mater.* **2003**, *15*, 2684–2686.

(65) Zhao, Y.; Wasielewski, M. R. *Tetrahedron Lett.* **1999**, *40*, 7047–7050.

(66) Sivamurugan, V.; Kazlauskas, K.; Jursenas, S.; Gruodis, A.; Simokaitiene, J.; Grazulevicius, J. V.; Valiyaveettil, S. *J. Phys. Chem. B* **2010**, *114*, 1782–1789.

(67) Qiu, W.-F.; Chen, S.-Y.; Sun, X.-B.; Liu, Y.-Q.; Zhu, D. *Org. Lett.* **2006**, *8*, 867–870.

(68) Zhan, X.; Tan, Z. A.; Zhou, E.; Li, Y.; Misra, R.; Grant, A.; Domercq, B.; Zhang, X.-H.; An, Z.; Zhang, X.; Barlow, S.; Kippelen, B.; Marder, S. R. *J. Mater. Chem.* **2009**, *19*, 5794–5803.

(69) Rohr, U.; Kohl, C.; Müllen, K.; van de Craats, A.; Warman, J. *J. Mater. Chem.* **2001**, *11*, 1789–1799.

(70) Rohr, U.; Schlichting, P.; Böhm, A.; Gross, M.; Meerholz, K.; Bräuchle, C.; Müllen, K. *Angew. Chem., Int. Ed.* **1998**, *37*, 1434–1437.

(71) An, Z.; Yu, J.; Jones, S. C.; Barlow, S.; Domercq, B.; Kippelen, B.; Marder, S. R. *J. Mater. Chem.* **2009**, *19*, 6688–6698.

(72) Jiang, W.; Li, Y.; Yue, W.; Zhen, Y.-G.; Qu, J.-Q.; Wang, Z.-H. *Org. Lett.* **2010**, *12*, 228–231.

(73) Qian, H.-L.; Wang, Z.-H.; Yue, W.; Zhu, D.-B. *J. Am. Chem. Soc.* **2007**, *129*, 10664–10665.

(74) Qian, H.-L.; Negri, F.; Wang, C.-R.; Wang, Z.-H. *J. Am. Chem. Soc.* **2008**, *130*, 17970–17976.

(75) Zhen, Y.-G.; Wang, C.-R.; Wang, Z.-H. *Chem. Commun.* **2010**, *46*, 1926–1928.

(76) Nakazono, S.; Easwaramoorthi, S.; Kim, D.; Shinokubo, H.; Osuka, A. *Org. Lett.* **2009**, *11*, 5426–5429.

(77) Nakazono, S.; Imazaki, Y.; Yoo, H.; Yang, J.; Sasamori, T.; Tokitoh, N.; Cedric, T.; Kageyama, H.; Kim, D.; Shinokubo, H.; Osuka, A. *Chem.—Eur. J.* **2009**, *15*, 7530–7533.

(78) Gsänger, M.; Oh, J. H.; Könemann, M.; Höffken, H. W.; Krause, A.-M.; Bao, Z.; Würthner, F. *Angew. Chem., Int. Ed.* **2010**, *49*, 740–743.

(79) Langhals, H.; Karolin, J.; Johansson, L. B.-Å. *J. Chem. Soc., Faraday Trans.* **1998**, *94*, 2919–2922.

(80) Oliveira, S. L.; Corrêa, D. S.; Misoguti, L.; Constantino, C. J. L.; Aroca, R. F.; Zilio, S. C.; Mendonça, C. R. *Adv. Mater.* **2005**, *17*, 1890–1893.

(81) Sadrai, M.; Hadel, L.; Sauers, R. R.; Husain, S.; Krogh-Jesperson, K.; Westbrook, J. D.; Bird, G. R. *J. Phys. Chem.* **1992**, *96*, 7988–7996.

(82) Corrêa, D. S.; Oliveira, S. L.; Misoguti, L.; Zilio, S. C.; Aroca, R. F.; Constantino, C. J. L.; Mendonça, C. R. *J. Phys. Chem. A* **2006**, *110*, 6433–6438.

(83) Würthner, F.; Thalacker, C.; Diele, S.; Tschierske, C. *Chem.—Eur. J.* **2001**, *7*, 2245–2253.

(84) Chao, C.-C.; Leung, M.-K.; Su, Y. O.; Chiu, K.-Y.; Lin, T.-H.; Shieh, S.-J.; Lin, S.-C. *J. Org. Chem.* **2005**, *70*, 4323–4231.

(85) Huang, J.; Wu, Y.; Fu, H.; Zhan, X.; Yao, J.; Barlow, S.; Marder, S. R. *J. Phys. Chem. A* **2009**, *113*, 5039–5046.

(86) Huang, J.; Fu, H.?B.; Wu, Y.?S.; Chen, S.?Y.; Shen, F.?G.; Zhao, X.?H.; Liu, Y.?Q.; Yao, J.?N. *J.?Phys. Chem. C* **2008**, *112*, 2689–2696.

(87) Zhou, E.; Tajima, K.; Yang, C.; Hashimoto, K. *J.?Mater. Chem.* **2010**, *20*, 2362–2368.

(88) Chen, Z.?H.; Zheng, Y.; Yan, H.; Facchetti, A. *J.?Am. Chem. Soc.* **2009**, *131*, 8–9.

(89) Hou, J.; Zhang, S.; Chen, T.?L.; Yang, Y. *Chem. Commun* **2008**, 6034–6036.

(90) Adachi, M.; Nagao, Y. *Chem. Mater.* **2001**, *13*, 662–669.

(91) Gómez, R.; Veldman, D.; Blanco, R.; Seoane, C.; Segura, J. L.; Janssen, R. A. J. *Macromolecules* **2007**, *40*, 2760–2772.

(92) Adachi, M.; Murata, Y.; Nakamura, S. *J. Phys. Chem.* **1995**, *99*, 14240–14246.

(93) De Boni, L.; Constantino, C. J. L.; Misoguti, L.; Aroca, R. F.; Zilio, S. C.; Mendonça, C. R. *Chem. Phys. Lett.* **2003**, *371*, 744–747.

(94) Lukas, A. S.; Zhao, Y.; Miller, S. E.; Wasielewski, M. R. *J. Phys. Chem. B* **2002**, *106*, 1299–1306.

(95) Salbeck, J.; Kunkely, H.; Langhals, H.; Saalfrank, R. W.; Daub, J. *Chimia* **1989**, *43*, 6–9.

(96) Bullock, J. E.; Vagnini, M. T.; Ramanan, C.; Co, D. T.; Wilson, T. M.; Dicke, J. W.; Marks, T. J.; Wasielewski, M. R. *J. Phys. Chem. B* **2010**, *114*, 1794–1802.

(97) Hayes, R. T.; Wasielewski, M. R.; Gosztola, D. *J. Am. Chem. Soc.* **2000**, *122*, 5563–5567.

(98) Ford, W. E.; Hiratsuka, H.; Kamat, P. V. *J. Phys. Chem.* **1989**, *93*, 6692–6696.

(99) Tauber, M. J.; Kelley, R. F.; Giaimo, J. M.; Rybtchinski, B.; Wasielewski, M. R. *J. Am. Chem. Soc.* **2006**, *128*, 1782–1783.

(100) van der Boom, T.; Hayes, R. T.; Zhao, Y.; Bushard, P. J.; Weiss, E. A.; Wasielewski, M. R. *J. Am. Chem. Soc.* **2002**, *124*, 9582–9590.

(101) Hädicke, E.; Graser, F. *Acta Crystallogr., Sect. C* **1986**, *42*, 195–198.

(102) Hädicke, E.; Graser, F. *Acta Crystallogr., Sect. C* **1986**, *42*, 189–195.

(103) Zugenmaier, P.; Duff, J.; Bluhm, T. L. *Cryst. Res. Technol* **2000**, *35*, 1095–1115.

(104) Hirose, Y.; Kahn, A.; Aristov, V.; Soukiassian, P.; Bulovic, V.; Forrest., S. R. *Phys. Rev. B* **1996**, *54*, 13748–13758.

(105) Scholz, M.; Schmidt, R.; Krause, S.; Schöll, A.; Reinert, F.; Würthner, F. *Appl. Phys. A: Mater. Sci. Process* **2009**, *95*, 285–290.

(106) Oh, J. H.; Liu, S.; Bao, Z.; Schmidt, R.; Würthner, F. *Appl. Phys. Lett.* **2007**, *91*, 212107.

(107) Sijibesma, R. P.; Meijer, E. W. *Chem. Commun.* **2003**, 5–16.

(108) Wang, W.; Han, J. J.; Wang, L.-Q.; Li, L.-S.; Shaw, W. J.; Li, A. D. Q. *Nano Lett.* **2003**, *3*, 455–458.

(109) You, C. C.; Würthner, F. *J. Am. Chem. Soc.* **2003**, *125*, 9716–9725.

(110) Würthner, F.; Thalacker, C.; Sautter, A. *Adv. Mater.* **1999**, *11*, 754–758.

(111) Wang, W.; Wan, W.; Zhou, H. H.; Niu, S. Q.; Li, A. D. Q. *J. Am. Chem. Soc.* **2003**, *125*, 5245–5249.

(112) Dobrawa, R.; Kurth, D. G.; Würthner, F. *Polym. Prepr.* **2004**, *45*, 378–379.

(113) Dobrawa, R.; Würthner, F. *Chem. Commun.* **2002**, 1878–1879.

(114) Shoaee, S.; Clarke, T. M.; Huang, C.; Barlow, S.; Marder, S. R.; Heeney, M.; McCulloch, I.; Durrant, J. R. *J. Am. Chem. Soc.* **2010**, *132*, 12919–12926.

(115) Kelley, R. F.; Shin, W. S.; Rybtchinski, B.; Sinks, L. E.; Wasielewski, M. R. *J. Am. Chem. Soc.* **2007**, *129*, 3173–3181.

(116) Odom, S. A.; Kelley, R. F.; Ohira, S.; Ensley, T. R.; Huang, C.; Padilha, L. A.; Webster, S.; Barlow, V. C. S.; Hagan, D. J.; Van Stryland, E. W.; Brédas, J.-L.; Anderson, H. L.; Wasielewski, M. R.; Marder, S. R. *J. Phys. Chem. A* **2009**, *113*, 10826–100832.

(117) Muthukumaran, K.; Loewe, R. S.; Kirmaier, C.; Hindin, E.; Schwartz, J. K.; Sazanovich, I. V.; Diers, J. R.; Bocian, D. F.; Holten, D.; Lindsey, J. S. *J. Phys. Chem. B* **2003**, *107*, 3431–3442.

(118) Kirmaier, C.; Hindin, E.; K., J.; Schwartz; Sazanovich, I. V.; Diers, J. R.; Muthukumaran, K.; Taniguchi, M.; Bocian, D. F.; Lindsey, J. S.; Holten, D. *J. Phys. Chem. B* **2003**, *107*, 3443–3454.

(119) Colvin, M. T.; Giacobbe, E. M.; Cohen, B.; Miura, T.; Scott, A. M.; Wasielewski, M. R. *J. Phys. Chem. A* **2010**, *114*, 1741–1748.

(120) Giacobbe, E. M.; Mi, Q.; Colvin, M. T.; Cohen, B.; Ramanan, C.; Scott, A. M.; Marks, T. J.; Ratner, M. A.; Wasielewski, M. R. *J. Am. Chem. Soc.* **2009**, *131*, 3700–3712.

(121) Cha, M.; Sariciftci, N. S.; Heeger, A. J.; Hummelen, J. C.; Wudl, F. *Appl. Phys. Lett.* **1995**, *67*, 3850–3852.

(122) Spangler, C. W. *J. Mater. Chem.* **1999**, *9*, 2013–2020.

(123) Chi, S.-H.; Hales, J. M.; Cozzuol, M.; Ochoa, C.; Fitzpatrick, M.; Perry, J. W. *Opt. Express* **2009**, *17*, 22062–22072.

(124) Defining EA as the energy change for the process PDI + e⁻ → PDI•⁻.

(125) Ostrick, J. R.; Dodabalapur, A.; Torsi, L.; Lovinger, A. J.; Kwock, E. W.; Miller, T. M.; Galvin, M.; Berggren, M.; Katz, H. E. *J. Appl. Phys.* **1997**, *81*, 6804–6808.

(126) Horowitz, G. K., F.; Spearman, P.; Fichou, D.; Nogues, C.; Pan, X.; Garnier, F. *Adv. Mater.* **1996**, *8*, 242–244.

(127) Tatemichi, S.; Ichikawa, M.; Koyama, T.; Taniguchi, Y. *Appl. Phys. Lett.* **2006**, *89*, 112108.

(128) Malenfant, P. R. L.; Dimitrakopoulos, C. D.; Gelorme, J. D.; Kosbar, L. L.; Graham, T. O.; Curioni, A.; Andreoni, W. *Appl. Phys. Lett.* **2002**, *80*, 2517–1519.

(129) Pandey, A. K.; Nunzi, J. M. *Appl. Phys. Lett.* **2007**, *90*, 263508.

(130) Warman, J. M.; de Haas, M. P.; Dicker, G.; Grozema, F. C.; Piris, J.; Debije, M. G. *Chem. Mater.* **2004**, *16*, 4600–4609.

(131) Chen, Z.; Debije, M. G.; Debaerdemaeker, T.; Osswald, P.; Würthner, F. *ChemPhysChem* **2004**, *5*, 137–140.

(132) Li, Y.; Tan, L.; Wang, Z.; Qian, H.; Shi, Y.; Hu, W. *Org. Lett.* **2008**, *10*, 529–532.

(133) Struijk, C. W.; Sieval, A. B.; Dakhorst, J. E. J.; Dijk, M. v.; Kimkes, P.; Koehorst, R. B. M.; Donker, H.; Schaafsma, T. J.; Picken, S. J.; van de Craats, A. M.; Warman, J. M.; Zuilhof, H.; Sudhlter, E. J. R. *J. Am. Chem. Soc.* **2000**, *122*, 11057–11066.

(134) Yu, W. L.; Pei, J.; Huang, W.; Heeger, A. J. *Adv. Mater.* **2000**, *12*, 828–831.

(135) Wang, Y.; Chen, Y.; Li, R.; Wang, S.; Su, W.; Ma, P.; Wasielewski, M. R.; Li, X.; Jiang, J. *Langmuir* **2007**, *23*, 5836–5842.

(136) Yan, H.; Chen, Z.-H.; Zheng, Y.; Newman, C.; Quinn, J.-R.; Dotz, F.; Kastler, M.; Facchetti, A. *Nature* **2009**, *457*, 679–681.

(137) Finlayson, C. E.; Friend, R. H.; Otten, M. B. J.; Schwartz, E.; Cornelissen, J. J. L. M.; Nolte, R. J. M.; Rowan, A. E.; Samorı, P.; Palermo, V.; Liscio, A.; Peneva, Kalina; Müllen, K.; Beljonne, S. T. *Adv. Funct. Mater.* **2008**, *18*, 1–9.

(138) The solid-state EA of the widely soluble C_{60} derivative PCBM can be estimated as ca. −3.7 eV using its electrochemical reduction potential of −1.08 V vs ferrocenium/ferrocene (ref 139). This value has been measured to be −3.8 to −3.9 eV using inverse photoelectron spectroscopy (refs 140 and 141).

(139) Kooistra, F. B.; Knol, J.; Kastenberg, F.; Popescu, L. M.; Verhees, W. J. H.; Kroon, J. M.; Hummelen, J. C. *Org. Lett.* **2007**, *9*, 551–554.

(140) Akaike, K.; Kanai, K.; Yoshida, H.; Tsutsumi, J. Y.; Nishi, T.; Sato, N.; Ouchi, Y.; Seki, K. *J. Appl. Phys.* **2008**, *104*, 023710.

(141) Guan, Z.-L.; Kim, J. B.; Wang, H.; Jaye, C.; Fischer, D. A.; Loo, Y.-L.; Kahn, A. *Org. Electron* **2010**, *11*, 1779–1783.

(142) Tang, C. W. *Appl. Phys. Lett.* **1986**, *48*, 183–185.

(143) Peumans, P.; Bulovic, V.; Forrest, S. R. *Appl. Phys. Lett.* **2000**, *76*, 2650–2652.

(144) Hiramoto, M.; Fujiwara, H.; Yokoyama, M. *J. Appl. Phys.* **1992**, *72*, 3781–3787.

(145) Whitlock, J. B.; Panayotatos, P.; Sharma, G. D.; Cox, M. D.; Sauers, R. R.; Bird, G. R. *Opt. Eng.* **1993**, *32*, 1921–1934.

(146) Arbour, C.; Armstrong, N. R.; Brina, R.; Collins, G.; Danziger, J.; Dodelet, J.-P.; Lee, P.; Nebesny, K. W.; Pankow, J.; Waite, S. *Mol. Cryst. Liq. Cryst.* **1990**, *183*, 307–320.

(147) Nakamura, J.-I.; Yokoe, C.; Murataa, K. *J. Appl. Phys.* **2004**, *96*, 6878–6884.

(148) Pandey, A. K.; Dabos-Seignon, S.; Nunzia, J.-M. *Appl. Phys. Lett.* **2006**, *89*, 113506.

(149) Rajaram, S.; Armstrong, P. B.; Kim, B. J.; Férchet, J. M. J. *Chem. Mater.* **2009**, *21*, 1775–1777.

(150) Li, J. L.; Dierschke, F.; Wu, J. S.; Grimsdale, A. C.; Müllen, K. *J. Mater. Chem.* **2006**, *16*, 96–100.

(151) Sharma, G. D.; Balraju, P; Mikroyannidis, J. A.; Stylianakis, M. M. *Sol. Energy Mater. Sol. Cells* **2009**, *93*, 2025–2028.

(152) Chirvase, D.; Chiguvare, Z.; Knipper, M.; Parisi, J.; Dyakonov, V.; Hummelen, J. C. *Synth. Met.* **2003**, *138*, 299–304.

(153) Darling, S. B. *Energy Environ. Sci.* **2009**, *2*, 1266–1273.

(154) Zhang, Q.; Cirpan, A.; Russell, T. P.; Emrick, T. *Macromolecules* **2009**, *42*, 1079–1082.

(155) Yuan, M.-C.; Su, M.-H.; Chiu, M.-Y.; Wei, K.-H. *J. Polym. Sci., Part A: Polym. Chem.* **2010**, *48*, 1298–1309.

(156) Koyuncu, S.; Zafer, C.; Koyuncu, F. B.; Aydin, B.; Can, M.; Sefer, E.; Ozdemir, E.; Icli, S. *J. Polym. Sci., Part A: Polym. Chem.* **2009**, *47*, 6280–6291.

(157) Liu, Y.; Yang, C.; Li, Y.; Li, Y.; Wang, S.; Zhuang, J.; Liu, H.; Wang, N.; He, X.; Li, Y.; Zhu, D. *Macromolecules* **2005**, *38*, 716–721.

(158) Liu, Y.; Wang, N.; Li, Y.; Liu, H.; Li, Y.; Xiao, J.; Xu, X.; Huang, C.; Cui, S.; Zhu, D. *Macromolecules* **2005**, *38*, 4880–4887.

(159) O'Regan, B.; Grätzel, M. *Nature* **1991**, *353*, 737–740.

(160) Tian, H.; Liu, P.-H.; Zhu, W.; Gao, E.; Wua, D.-J.; Cai, S. *Chem. Commun.* **2000**, *10*, 2708–2715.

(161) Shibano, Y.; Umeyama, T.; Matano, Y.; Imahori, H. *Org. Lett.* **2007**, *9*, 1971–1974.